applied sciences

MDPI

Article

Validation of a Simulink Model for Simulating the Two Typical Controlled Ventilation Modes of Intensive Care Units Mechanical Ventilators †

Paolo Tamburrano [1], Francesco Sciatti [1,*], Elia Distaso [1], Luigi Di Lorenzo [2] and Riccardo Amirante [1]

[1] Department of Mechanics, Mathematics and Management (DMMM), Polytechnic University of Bari, 70121 Bari, Italy, ; paolo.tamburrano@poliba.it (P.T.); elia.distaso@poliba.it (E.D.); riccardo.amirante@poliba.it (R.A.)
[2] Interdisciplinary Department of Medicine, University of Bari, 70121 Bari, Italy; luigi.dilorenzo@uniba.it
* Correspondence: francesco.sciatti@poliba.it
† This paper is an extended version of "Tamburrano, P.; De Palma, P.; Plummer, A.R.; Distaso, E.; Amirante, R. Simulink Modelling for Simulating Intensive Care Mechanical Ventilators. In Proceedings of the E3S Web of Conferences, Rome, 15/16 September 2020; Volume 197, p. 07007".

Abstract: Mechanical ventilators are vital components of critical care services for patients with severe acute respiratory failure. In particular, pressure- and volume-controlled mechanical ventilation systems are the typical modes used in intensive care units (ICUs) to ventilate patients who cannot breathe adequately on their own. In this paper, a Simulink model is proposed to simulate these two typical modes employed in intensive care lung ventilators. Firstly, these two modes of ventilation are described in detail in the present paper. Secondly, the suggested Simulink model is analysed: it consists of using well-established subroutines already present in Simulink through the Simscape Fluids (gas) library, to simulate all the pneumatic components employed in some commercial ICU ventilators, such as pressure reducing valves, pressure relief valves, check valves, tanks, ON\OFF and proportional directional valves, etc. Finally, the simulation results of both modes in terms of pressure, tidal volume, and inspired/expired flow are compared with the real-life quantitative trends taken from previously recorded real-life experiments in order to validate the Simulink model. The accuracy of the model is high, as the numerical predictions are in good agreement with the real-life data, the percentage error being less than 10% in most comparisons. In this way, the model can easily be used by manufacturers and start-ups in order to produce new mechanical ventilators in the shortest time possible. Moreover, it can also be used by doctors and trainees to evaluate how the mechanical ventilator responds to different patients.

Keywords: Simulink; VC-CMV; PC-CMV

Citation: Tamburrano, P.; Sciatti, F.; Distaso, E.; Di Lorenzo, L.; Amirante, R. Validation of a Simulink Model for Simulating the Two Typical Controlled Ventilation Modes of Intensive Care Units Mechanical Ventilators. *Appl. Sci.* **2022**, *12*, 2057. https://doi.org/10.3390/app12042057

Academic Editor: Alessandro de Sire

Received: 22 November 2021
Accepted: 31 January 2022
Published: 16 February 2022

1. Introduction

The world health crisis due to COVID-19 is unprecedented. Whilst the drive to find a vaccine has produced excellent results, a great number of people are still in intensive care and need specific treatment that is only available in specially equipped hospitals. Mechanical ventilators are often found within medical infrastructures; however, the excessive volume of patients as a result of the pandemic has meant that there simply are not enough of them to cope with the high demand [1–3]. Whilst it is clear that the level of hygiene in medical facilitates should be maintained at the highest level, there is also an urgent need to address the issue of air quality and thermal comfort in these establishments. The spread of the disease through the air and rapid transmission makes this an urgent priority.

In this context, a properly designed, installed, and operated building automation and control system is fundamental to attaining an energy efficient operation and optimal indoor conditions, in the structures shown in [4].

The mechanical ventilator is a vital component of critical care services for patients with severe acute respiratory failure as it provides the energy necessary to ensure adequate flow, pressure, and volume of gas in the alveoli during inspiration.

Modern mechanical ventilation exploits the concept of positive pressure ventilation, in which the mechanical ventilator allows the patient to inhale by applying an over atmospheric pressure to the airways of the patient, generating a positive pressure inside them that mechanically produces the current volume [5]. The ventilator can be connected to the patient's airway through an endotracheal tube (invasive mechanical ventilation) or through a face mask (non-invasive ventilation) [6].

A mechanical ventilator is a sophisticated electronic machine that replaces, either totally or partially, the mechanical functions of the respiratory system when it becomes unable to perform its task because of critical conditions due to illness or surgical procedures [7]. It consists primarily of two blocks. The first is a pneumatic unit, composed of directional valves, check valves, pressure regulators, filters, tanks, pressure transducers, and flow rate sensors, and is connected to the patient's lungs through a series of tubes. The second is an electronic unit that performs logic operations, and allows the doctor to set the conditions and parameters of the values of interest and that trigger alarms if the patient is in danger [5]. Modern ventilators use closed-loop control to keep the inspiration and expiration pressure, or the inspiration flow, constant in the face of the changing conditions of the patient [7,8]. The control system of the ICU ventilator allows the operators/doctors to set different ventilation modes according to the required parameters, such as, respiratory rate (RR), peak inspiratory flow rate (I_{pf}), the percentage of inhaled oxygen (FiO_2), inspiratory: expiratory ratio (I:E), tidal volume (V_T), peak of inspiratory pressure (PIP), and the positive end-expiratory pressure (PEEP) [9,10]. At least three of these parameters have to be set independently in order to achieve the required ventilation mode [11].

The pneumatic schemes of commercially available ventilators for ICUs can present some variations depending on the design adopted by the manufacturer. Most manufacturers have made the pneumatic circuit of their ventilators available as part of their published technical information in response to the emergency caused by the spread of COVID-19. Ventilators for intensive care units include: the Siaretron 4000, produced by Siare Engineering; the Galileo ventilator, produced by Hamilton Medical [12]; the Dräger Infinity V500 intensive care ventilator, produced by Dräger Medical AG & Co [13]; the Aisys CS^2, produced by GE Healthcare [14]; the Puritan Bennett 800, produced by Medtronic [15].

In order to address the emergency situation caused by the pandemic, the Medicine and Healthcare products Regulatory Agency (MHRA) in the United Kingdom, and the Food and Drug Administration (FDA) in the US, have recently published guidelines on the technical specifications that ventilators must possess in order to be used in hospitals during the COVID-19 outbreak [16]. An extensive review of the expected parameters, performance, and the mode of operation of mechanical ventilators is provided in [17,18]. To meet this challenge, researchers, engineers, doctors, and scientists from around the world undertook the task of designing easily useable mechanical ventilators, such as in [19,20]. Academic institutions, industries, and several manufacturers, such as GM, Ford, Dyson, Rolls-Royce, and Tesla have made efforts to adapt their manufacturing facilities to create ventilators for the very first time [1]. In addition to this, strategies have been proposed for the sharing of a ventilator between two patients (co-venting) [3]. Moreover, in [21], an overview of the available data regarding the respiratory mechanics and mechanical ventilation settings for patients admitted to ICUs due to COVID-19 is illustrated. In particular, the mode of ventilation used within the first 24 h in ICUs was the "pressure-controlled continuous mandatory ventilation (PC-CMV)" mode for 52%, and the "volume-controlled continuous mandatory ventilation (VC-CMV)" mode for 19% [22]. The values of tidal volume varied from 5.6 to 7.5 mL/kg [23], the plateau pressure (P_{plt}) ranged from 20.5 to 31 cmH_2O [24,25], the PEEP ranged from a minimum of 9 to a maximum of 16.5 cmH_2O [23,26], the respiratory rate (RR) ranged from 20 to 33 breaths/min [23,26,27], and the compliance of the respiratory system (C_{RS}) showed wide variations, ranging from 24 to 49 mL/cmH_2O [24,25].

Under this scenario, the aim of this paper is to propose an accurate simulation modelling platform and to validate it for the typical modes of ventilation in ICU mechanical ventilators, namely the "volume-controlled continuous mandatory ventilation (VC-CMV)" mode and the "pressure-controlled continuous mandatory ventilation (PC-CMV)" mode. The numerical model, which simulates the interaction between human lungs and mechanical ventilators, could prove to be extremely beneficial to doctors when making vital decisions, as the information can easily be seen on a simple graphical interface.

The concept of computer-aided prototyping of a mechanical system, performed in a simulation environment that permits the modelling of complex scenarios, such as Matlab/Simulink, has been used in a wide spectrum of studies, ranging from the simulation of the dynamic vehicles to exoskeleton design for rehabilitation [28–33]. Therefore, by automating the process, it is possible to control both the ventilation modes and the parameters based on the patient's condition. This has been an area of great scientific interest, especially since the advent of COVID-19.

In [34], Matlab/Simulink and the Simscape libraries were used to create a simulation model in order to study the interaction between human lungs and mechanical ventilators. The model comprised the patient's lungs, the ventilator device with valves and tubes, as well as a pressure-targeted ventilator controller. The patient's lungs were simulated as a piston moving inside a cylinder, the lung compliance was simulated as a spring, the airway resistance as a damper, and the inspiratory and expiratory tubes and the trachea as pipes. A closed-loop control was used to control the mechanical ventilation process with a pre-set value of flow supplied to the patient. Thus, the variables were transferred to the embedded software system, where the calculation of ventilatory parameters and variables was obtained.

In [35], both numerical simulations and experimental tests on rats were carried out in order to show the interaction between the ventilator and lung model. Firstly, the lung mechanics and mechanical ventilator were modeled in Matlab/Simulink, and three different lung models were used to represent the rat. Pressure waveforms, using the VC-CMV mode, were calculated for all models for three different airway resistance values using the same lung compliance value. Secondly, a mechanical ventilator prototype was designed and controlled via fuzzy control through the LabVIEW 2010 academic software.

In comparison to the work conducted in [34,35], in which only the VC-CMV mode with a square flow pattern was simulated, in the present work, we show that simulations of different ventilation modes, i.e., the VC-CMV mode and PC-CMV mode, with different flow and pressure patterns, respectively, can be obtained using the proposed numerical codes.

In [3], MathWorks® Simscape foundational blocks were used to create a model in order to evaluate the sharing of a ventilator between two patients (co-venting). However, in contrast to our models, the system connecting the ventilator to the two patients and their lungs was simulated as an electrical circuit. Thus, the tubes were simulated as resistors, the lung and chest wall as a capacitor, the pressure source as a voltage source, a one-way valve as a diode, and an open/close valve as a switch. Furthermore, only the PC-CMV mode with constant square pressure pattern was simulated.

In [36], the electromechanical lung simulator xPULM, a respiratory simulation system presented in [37], was used to test the interaction between a patient and a ventilator. The simulator acted as a ventilated patient and replicated spontaneous sinusoidal breathing, while supported by different modes of assisted ventilation.

In addition, flow simulation produced by two proposed designs of low-cost mechanical ventilators was investigated in [38] during the VC-CMV and PC-CMV modes.

In this work, the Simulink model is composed of blocks from the Simscape Fluids (gas) library [39,40], which allowed us to simulate the pneumatic circuit and all the components of the ventilator. Conversely, the patient's lungs and the trachea are reproduced in the model by setting the lung compliance and the resistance of the respiratory system, respectively. In this way, the fundamental parameters and variables of the mechanical ventilation can easily be calculated and used by doctors to evaluate how the mechanical ventilator

responds to different patients. Furthermore, the model can also be used by start-ups and manufacturers, both to accelerate the production of new mechanical ventilators and to predict their performance.

2. Mechanical Ventilation Modes

A mode of mechanical ventilation may be defined, in general, as a predetermined pattern of patient–ventilator interaction [41]. In respiratory mechanics, it is useful to think of patient–ventilator interactions in terms of a mechanical system consisting firstly of a resistive element (a rigid tube) followed by an elastic element (a balloon), which in turn are connected to a mechanical ventilator (a piston), as shown in Figure 1.

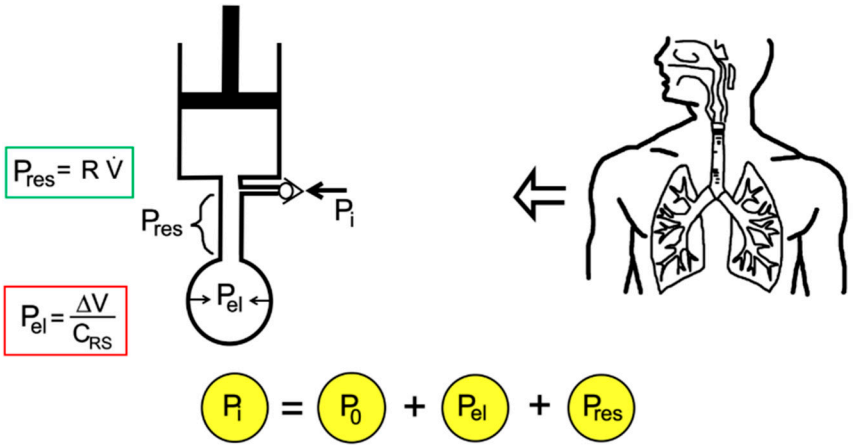

Figure 1. Mono-compartment model of the respiratory system connected to ventilator using mechanical analogues.

An in-series mechanical arrangement means that at any time (t), the pressure that is applied to the tube inlet (the airway pressure, $P_i(t)$) is equal to the sum of three pressures, the initial alveolar pressure at the beginning of the inspiration (P_0), which can be atmospheric pressure or greater than atmospheric pressure (called positive end-expiratory pressure, PEEP), an elastic pressure ($P_{el}(t)$), and a resistive pressure ($P_{res}(t)$):

$$P_i(t) = P_0 + P_{el}(t) + P_{res}(t), \quad (1)$$

The elastic pressure is the pressure needed to expand the lungs and chest wall, whereas the resistive pressure is that needed to generate a certain gas flow rate within the airways. These two pressures can then be expressed as a function of the parameters of respiratory mechanics, namely the elastance of the respiratory system (E_{RS}) and the airway resistance to flow ($R_{insp/exp}$). Therefore, E_{RS} reflects the elastic characteristics of the respiratory system and is the inverse of the compliance of the respiratory system, $C_{RS} = 1/E_{RS}$. The inspiratory resistance (R_{insp}) describes the opposition to a flow of gas entering the respiratory system during inspiration, and is primarily made up of the resistance of the airways and the endotracheal tube. The expiratory resistance (R_{exp}) is higher than the inspiratory resistance due to the shape of the airway tree. Therefore, assuming linear system behaviour, as shown in [7], and knowing the parameters of respiratory mechanics, the inlet pressure–time profile can be computed for any piston stroke volume (V) and flow ($\dot{V}$) setting:

$$P_i(t) = P_0 + \frac{V(t)}{C_{RS}} + R_{insp/exp}\,\dot{V}(t), \quad (2)$$

Let us then move on to the concepts of breath and breath sequence. A breath, which can be mandatory, assisted, or spontaneous, is one cycle of positive flow (inspiration) and negative flow (expiration) defined in terms of the flow–time curve. A mandatory breath is a breath in which the start or end of inspiration (or both) is determined by the ventilator,

independent of the patient's condition. An assisted breath is a breath in which the ventilator does some portion of the work of breathing. A spontaneous breath is a breath in which the patient him/herself initiates and finishes the inspiration, independent of any ventilator settings for inspiratory and expiratory times. Thus, based on these types of breath, we can speak of different types of breath sequence, namely continuous mandatory ventilation (CMV), continuous spontaneous ventilation (CSV), and intermittent mandatory ventilation (IMV). The former is also commonly known as assist control (when the breaths are patient-triggered), and is a breath sequence in which spontaneous breaths are not permitted between mandatory breaths. The second is a breath sequence in which all the breaths are spontaneous. The latter is a breath sequence in which spontaneous breaths are allowed between mandatory breaths [41]. It can therefore be understood that the total airway pressure ($P_i(t)$) needed to provide a respiratory act is given by the sum of the pressure developed by the respiratory muscles and the pressure developed by the ventilator:

$$P_i(t) = P_{vent}(t) + P_{musc}(t) = P_0 + \frac{V(t)}{C_{RS}} + R_{insp/\,exp}\,\dot{V}(t) \quad (3)$$

This is called the equation of motion for the respiratory system, and points out the parameters that define the respiratory mechanics (C_{RS}, R_{insp}, R_{exp}), and the variables adjustable by the operator on the machine (P, V, $\dot{V}$) and that, therefore, represent the control variables. We can then construct a mode of ventilation using these three basic components: (1) the control variable, (2) the breath sequence, and (3) the operational algorithm. The last is the feedback control system used by mechanical ventilators to deliver specific ventilatory patterns. Seven different control types have been evolved to date; the simplest is set-point control, in which the output of the ventilator automatically matches a constant operator pre-set input value [42]. Indeed, modern mechanical ventilators use closed-loop control to maintain consistent pressure and flow waveforms in the face of changing patient/system conditions [7,8]. Therefore, given two possible control variables (volume, pressure) and three breath sequences (CMV, IMV, CSV), there are five possible mechanical ventilation modes (Table 1).

Table 1. Mechanical ventilation modes, adapted from [42].

Control Variables	Breath Sequence	Ventilation Mode	Acronym
Pressure	CSV	Pressure Support	PS-CSV
	CMV	Pressure Control	PC-CMV
	IMV	Pressure Control	PC-IMV
Flow–Volume	CMV	Volume Control	VC-CMV
	IMV	Volume Control	VC-IMV

Thus, whereas modern lung ventilators offer different operating modes to be adopted according to the specific needs of the patient, the basic criterion for the choice of ventilation model is based on the patient's ability to breathe autonomously.

Once the control variable has been established (the main variable that the ventilator control circuit manipulates to cause inspiration), the ventilator needs more information to know how to handle the inspiratory and expiratory phase, as breathing is a periodic event. This is possible through the application of phase variables. These are essential in order to define how the ventilator starts (trigger variable), maintains (limit variable), and ends (cycle variable) the inspiratory phase, and how it behaves during the expiration phase (baseline variable). Thus, a particular variable is measured and used to initiate, maintain, and terminate each phase. In this context, pressure, volume, flow, and time are referred to as phase variables. In fact, depending on how the phase variables are distributed between ventilator and patient, it is possible to distinguish the ventilation mode, as shown in Table 2.

Table 2. Classification of the mechanical ventilation modes based on phase variables, adapted from [5].

Ventilation Mode	Trigger Variable	Limit Variable	Cycle Variable
Controlled	Ventilator	Ventilator	Ventilator
Assisted–Controlled	Patient	Ventilator	Ventilator
Supported	Patient	Ventilator	Patient
Spontaneous	Patient	Patient	Patient

This paper focuses on the controlled mode, for which the mechanical ventilator performs 100% of the respiratory work, as these are the modes used on COVID-19 patients within the first 24 h of ICU stay.

2.1. VC-CMV Mode

In volume-controlled ventilation, the patient receives a pre-set tidal volume (V_T) determined by the pre-set inspiratory peak flow rate (I_{pf}) over a set inspiratory time (T_i).

$$V_T = I_{pf}\, T_i, \tag{4}$$

This mode is used when a precise minute ventilation is therapeutically essential to the care of the patient [43]. Minute ventilation is entirely determined by the ventilator settings, as the patient is unable to initiate spontaneous breaths. Therefore, the doctor/clinician selects tidal volume (V_T), respiratory rate (RR), and peak inspiratory flow rate (I_{pf}) (independent variables), in addition to PEEP, FiO_2, and pressure airway limit ($P_{aw,limit}$). Based on these independent variables, the ventilator automatically calculates the dependent variables, namely expiration time (T_e), and then inspiration/expiration ratio (I:E) and total time cycle (TCT).

$$T_e = \frac{60}{RR} - T_i, \tag{5}$$

$$I:E = \frac{T_i}{T_e}, \tag{6}$$

$$TCT = T_i + T_e, \tag{7}$$

Airway pressures (peak, plateau, and mean) are not directly adjusted, and are dependent on the equation of motion for the respiratory system through the patient variables (C_{RS}, R_{insp}, R_{exp}). The correlation between independent, dependent, and patient variables in VC-CMV mode is shown in Figure 2.

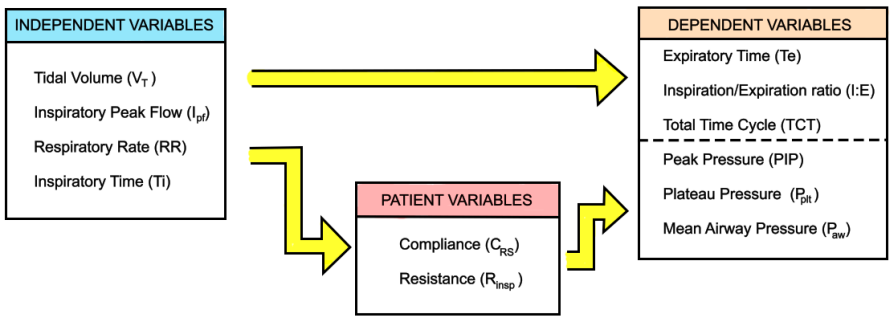

Figure 2. Independent and dependent variables in VC-CMV mode, adapted from [5].

The airway pressure measured during the inspiration pause (absence of flow) is referred to as the plateau pressure (P_{plt}), and is a measure of the alveolar pressure, as the

pressure drop due to airway resistance is zero at zero flow. This is based on the equation of motion for the respiratory system:

$$P_{plt} = P_0 + \frac{V_T}{C_{RS}}, \tag{8}$$

On the other hand, the inspiratory resistance (R_{insp}), which can be calculated only in VC-CMV mode when the inspiratory flow pattern is constant (square), allows the machine to evaluate the PIP as follows:

$$PIP = P_{plt} + R_{insp}I_{pf}, \tag{9}$$

Mean airway pressure, which is defined as the average pressure at the airway opening over a given time interval [44], is generally higher for pressure-controlled modes than volume-controlled modes (at the same tidal volume) due to the differences in the shapes of the airway pressure waveforms. Indeed, it is evaluated as:

$$\overline{P}_{aw} = k(PIP - PEEP)\left(\frac{T_i}{T_i + T_e}\right) - PEEP \tag{10}$$

where (k = 1) for rectangular waveform and ($0.5 \leq k \leq 1$) for other waveforms.

Modern ICU ventilators provide graphic displays in two formats: waveforms and loops. Waveform displays show pressure, volume, and flow on the vertical axis, with time on the horizontal axis. Loop displays show one variable plotted against another (flow–volume or pressure–volume). Breaths, during VC-CMV, can be machine-triggered (a) or patient-triggered (b) and the waveform displays are different, as shown in Figure 3.

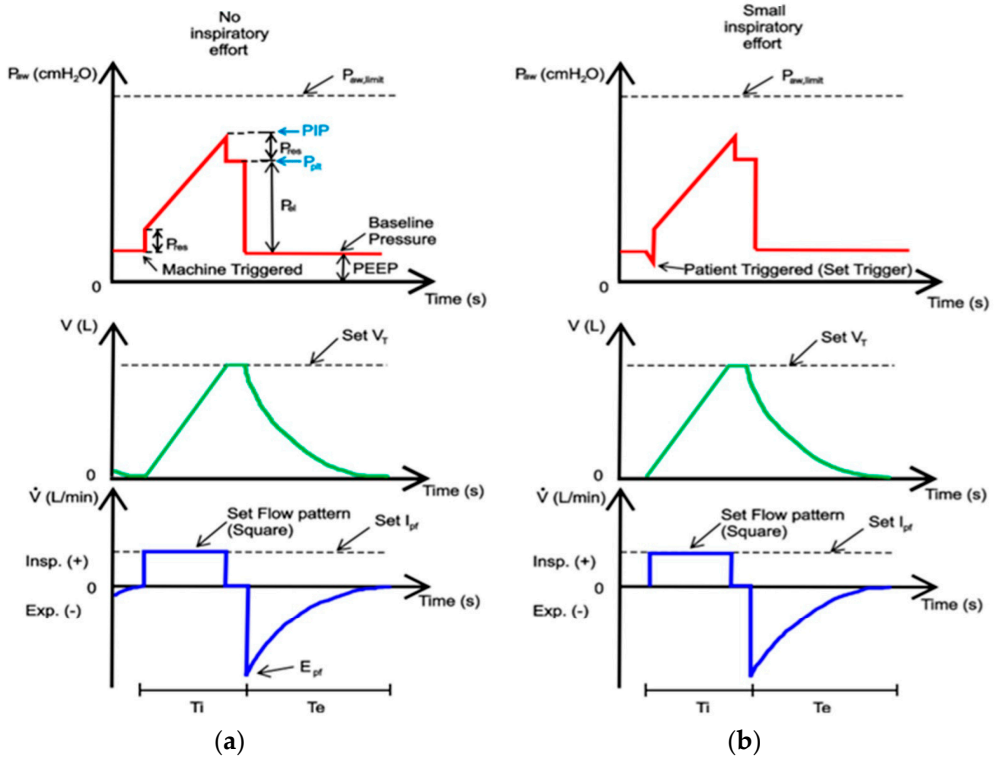

Figure 3. A display of pressure, volume, and flow waveforms during VC-CMV mode: (**a**) machine-triggered; (**b**) patient-triggered. The theoretical waveforms have been adapted from [44].

The area of the pressure curve under the baseline is proportional to the work the patient does on the ventilator, and the area above is the work the ventilator does on the patient.

If PIP is the same or greater than $P_{aw,limit}$, then the inspiratory flow is stopped, the inspiratory phase ends, and the ventilator emits an alarm. There are several causes of increased PIP, such as a reduction in lung compliance or an increase in airway resistance. Indeed, if R_{insp} increases, P_{res} increases on the same I_{pf}, and PIP increases; alternatively, if C_{RS} decreases (due to stiff lungs), then P_{el} increases on the same V_T, and PIP increases. In addition to this, during expiration, the increase in resistance (R_{exp}) causes a drop in peak expiratory flow (E_{pf}) and the expiration is prolonged. On the other hand, during expiration, the decrease in lung compliance generates an increase in peak expiratory flow (E_{pf}). All these effects are shown in Figure 4.

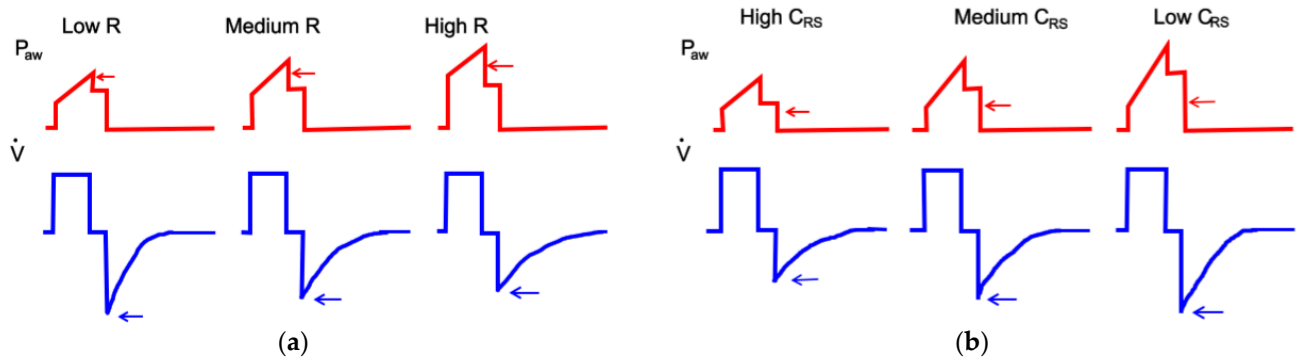

Figure 4. Effect of the increase in resistance airway (**a**) and decrease in lung compliance (**b**) during VC-CMV mode, adapted from [45].

Flow patterns that are typically used in volume-controlled mode are shown in Figure 5.

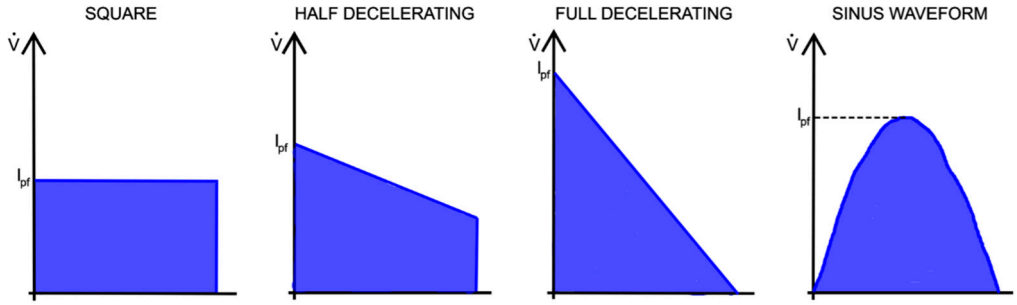

Figure 5. Various flow patterns typically used in VC-CMV mode.

During constant flow, another important parameter is the stress index. This is determined by the slope change in the airway pressure curve when the volume is controlled by a square flow pattern, and is used to evaluate the elastic properties of the lungs [43]. Ideally, a stress index = 1 means normal filling during lung expansion, indicating that the airway pressure increases linearly during inhalation (compliance is constant throughout inspiration). Alternatively, a stress index > 1 indicates overdistention of the lungs, and, therefore, an increasing amount of pressure is required during inspiration because compliance decreases gradually (concavity of the upward curve). Finally, a stress index < 1 indicates lung recruitment, meaning that less pressure is needed to obtain the current volume during inspiration. This is because the compliance increases gradually (concavity of the downward curve). A conceptional illustration of the dynamic pressure–time curve with different stress indexes is shown in Figure 6.

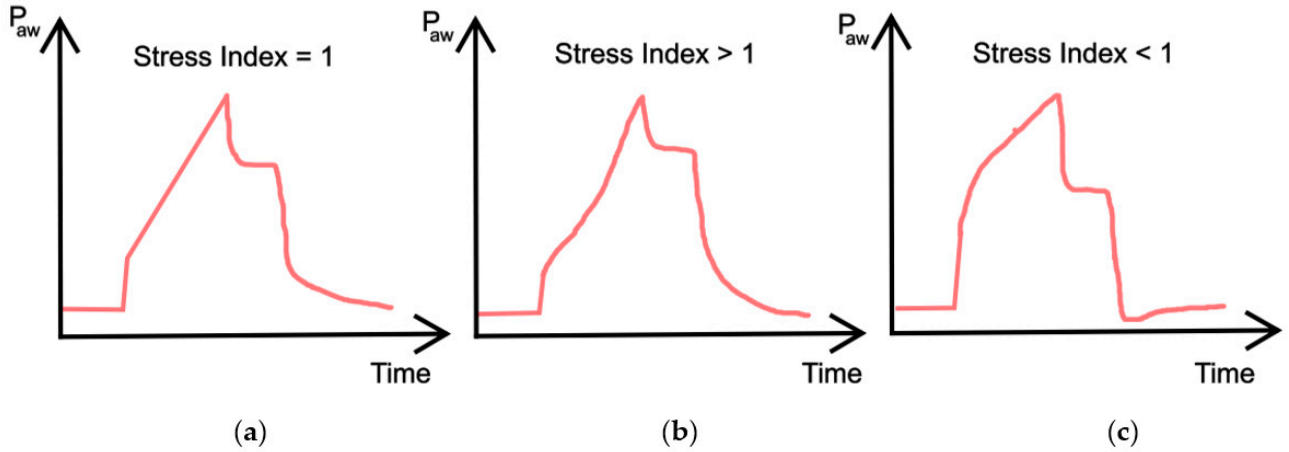

Figure 6. (**a**) Linear relationship between pressure and time indicating no recruitment or overdistention; (**b**) Concave curve indicating overdistention; (**c**) Convex curve indicating recruitment during the breath.

The most common units of measurement describing flow are litres per minute (L/min) or litres per second (L/s) in pulmonary physiology, whereas the unit relating to pressure is cmH_2O [43].

2.2. PC-CMV Mode

Similar to the VC-CMV mode, the PC-CMV mode can be used as a basic mode of ventilatory support. Again, in PC-CMV mode the goal is to maintain an adequate minute ventilation. However, this time the control variable is the airway pressure. Therefore, the doctor/clinician selects airway pressure (P_{aw}), respiratory rate (RR), and inspiration time (T_i) (independent variables), from which the machine calculates expiration time (T_e), inspiration/expiration ratio (I:E), and, through the patient variables (C_{RS}, R_{insp}), inspiratory peak flow (I_{pf}) and tidal volume (V_T) (dependent variables), as shown in Figure 7.

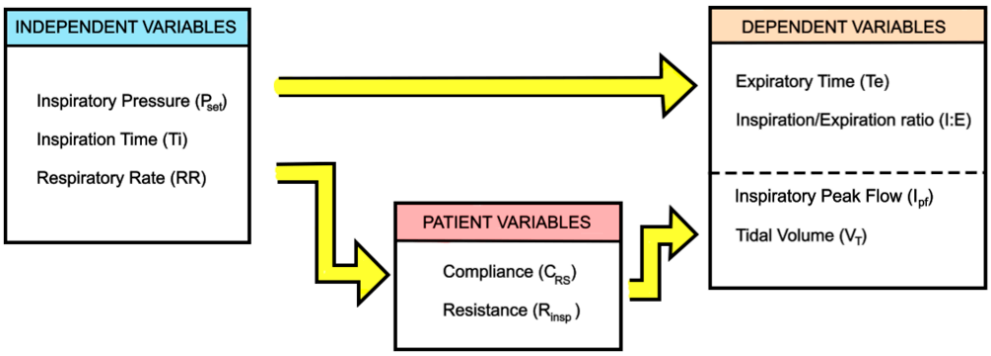

Figure 7. Independent and dependent variables in PC-CMV mode, adapted from [5].

In PC-CMV mode, inspiratory flow is a consequence of the ventilator's attempt to maintain a pre-set pressure waveform. The inspiratory flow is generated by the pressure gradient between the set pressure and the alveolar pressure (ΔP). Its maximum is at the beginning of inspiration when alveolar pressure is equal to PEEP:

$$\Delta P = P_{set} - PEEP, \quad (11)$$

This ΔP maximum allows the inspiratory flow to increase rapidly and to reach its peak (I_{pf}). Subsequently, as alveolar pressure increases gradually during inflation, ΔP decreases and, if the inspiration time (T_i) is long enough, the inspiratory flow exponentially drops to zero. This is due to the alveolar pressure reaching the value of the pressure set, and

the pressure gradient becomes null. The dynamics of the drop in flow depend on the inspiratory time constant (τ_i):

$$\tau_i = C_{RS}\, R_{insp}, \tag{12}$$

Therefore, this time $P_i(t)$ in the equation of motion for the respiratory system becomes constant (P_{set} = PIP). Using this equation, it is possible to evaluate the tidal volume and the inspiratory and expiratory flow, as follows:

$$V_T = \Delta P \cdot C_{RS}\left(1 - e^{-\frac{t}{\tau_i}}\right), \tag{13}$$

$$\dot{V}_I = \frac{\Delta P}{R_{insp}}\left(e^{-\frac{t}{\tau_i}}\right), \tag{14}$$

$$\dot{V}_E = \frac{\Delta P}{R_{exp}}\left(e^{-\frac{t}{\tau_e}}\right), \tag{15}$$

when in the Equations (14) and (15) the time is zero, then $\dot{V}_I = I_{pf}$ and $\dot{V}_E = E_{pf}$.

Again, breaths can be machine-triggered (a) or patient-triggered (b) in this mode, although the waveform displays are different, as shown Figure 8.

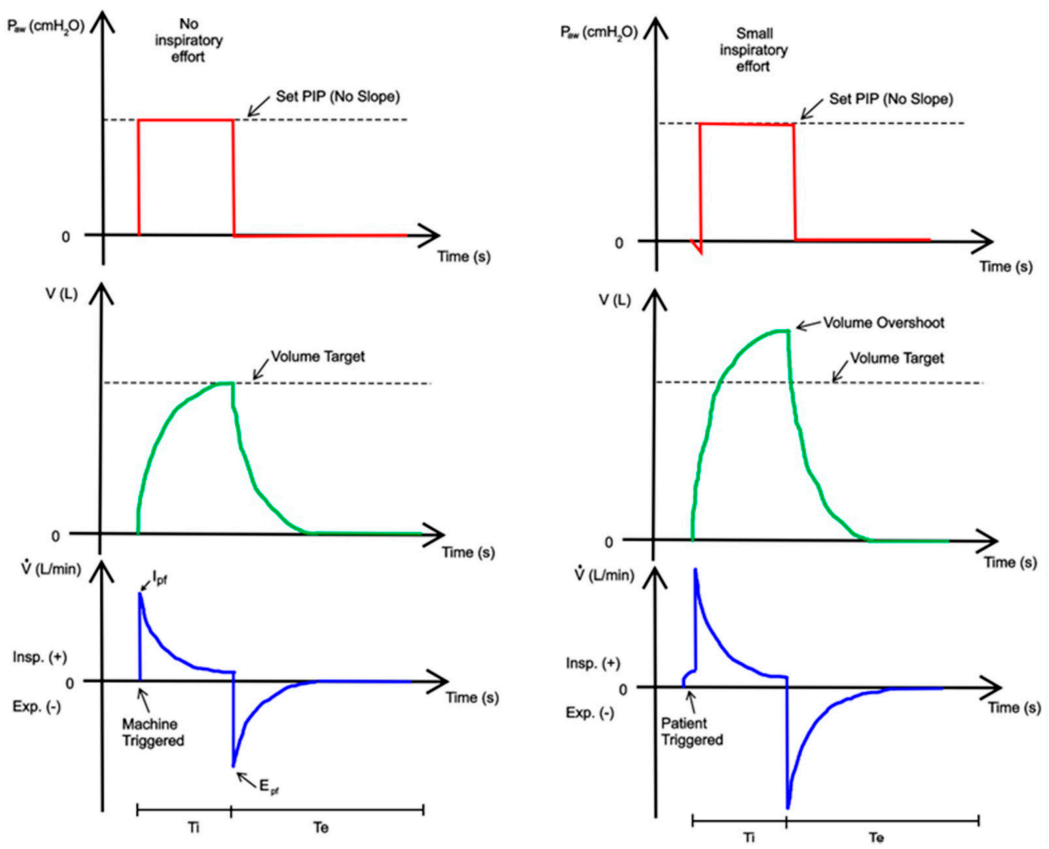

(**a**) (**b**)

Figure 8. A display of pressure, volume, and flow waveforms during PC-CMV mode: (**a**) machine-triggered; (**b**) patient-triggered. The theoretical waveforms have been adapted from [44].

In the PCV mode, the effects of changes in airway resistance and the compliance of respiratory system are very different. Indeed, during inspiration, if R_{insp} increases, I_{pf} decreases, T_i is prolonged, and P_{plt} decreases. If R_{insp} is very high, V_T decreases. The changes induced by the rise in R_{exp} during the expiratory phase of the cycle are identical to those observed in the VC-CMV mode. On the other hand, a decrease in C_{RS} causes the flow

to decelerate faster, the inspiratory pause is prolonged, and V_T is lowered. This produces faster expiration. All these effects are shown in Figure 9.

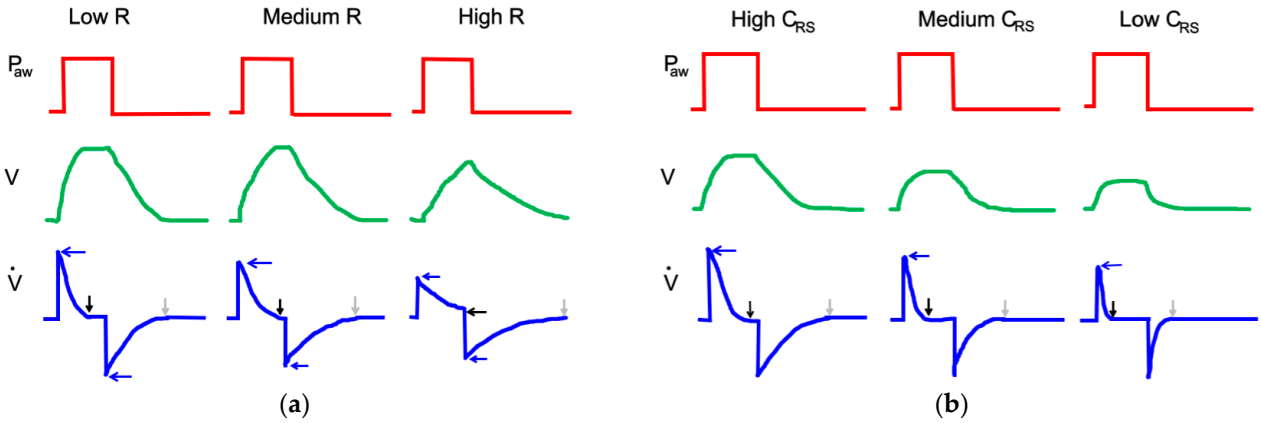

Figure 9. Effect of the increase in airway resistance (**a**) and decrease in lung compliance (**b**) during PC-CMV mode, adapted from [45].

Furthermore, in PC-CMV mode, inspiratory pressure pattern can be a square, a ramp, or an exponential rise. With the square pressure pattern, the inspiratory pressure instantly reaches the PIP and the flow is higher. Conversely, the slope of the ramp reduces the peak inspiratory flow (I_{pf}) and the tidal volume (V_t), and increases the length of inspiratory flow, as shown in Figure 10.

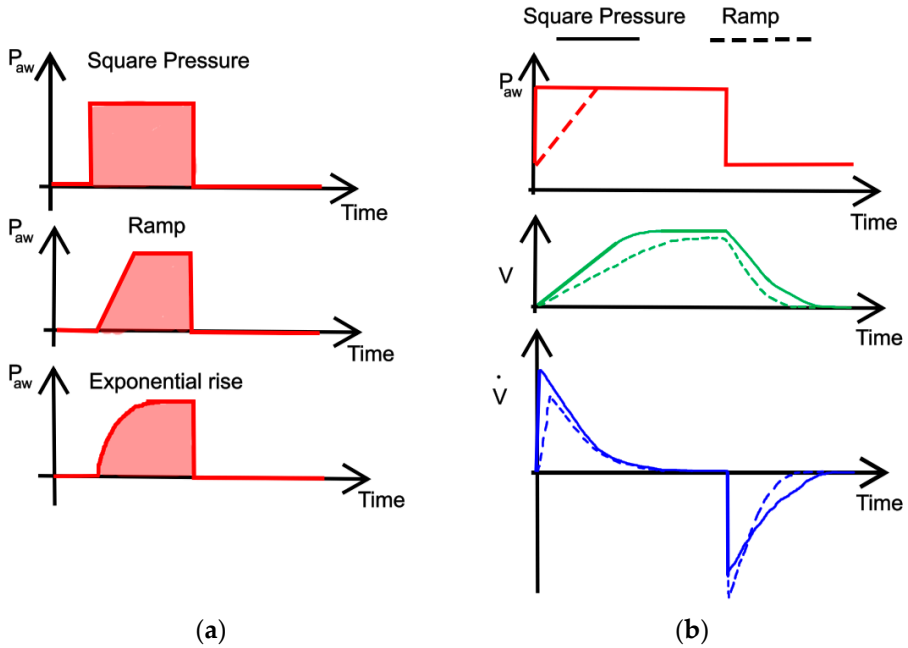

Figure 10. Various inspiratory pressure patterns typically used in PC-CMV mode (**a**) and comparison (**b**). The theoretical trends have been adapted from [46].

To sum up, the equations relating to the important parameters for the VC-CMV and PC-CMV modes are shown in Table 3.

Table 3. Equations relating the important parameters for VC-CMV and PC-CMV mode, adapted from [44].

Mode	Parameter	Symbol	Equation
VC-CMV	Tidal Volume (L)	V_T	$V_T = I_{pf}\, T_i$
	Mean Inspiratory Flow (L/s)	$\dot{V}_I$	$\dot{V}_I = \frac{60 V_T}{T_i}$
	Plateau Pressure (cmH_2O)	P_{plt}	$P_{plt} = P_0 + \frac{V_T}{C_{RS}}$
	Insp. Peak Pressure (cmH_2O)	PIP	$PIP = P_{plt} + R_{insp}\, I_{pf}$
PC-CMV	Tidal Volume (L)	V_T	$V_T = \Delta P\, C_{RS}\left(1 - e^{-\frac{t}{\tau_i}}\right)$
	Inspiratory Flow (L/s)	$\dot{V}_I$	$\dot{V}_I = \frac{\Delta P}{R_{insp}}\left(e^{-\frac{t}{\tau_i}}\right)$
	Pressure Gradient (cmH_2O)	ΔP	$\Delta P = PIP - PEEP$
Both modes	Total Cycle Time (s)	TCT	$TCT = T_i + T_e = \frac{60}{RR}$
	I:E ratio	I:E	$I:E = \frac{T_i}{T_e}$
	Inspiratory Time Constant (s)	τ_{insp}	$\tau_{insp} = R_{insp}\, C_{RS}$
	Expiratory Time constant (s)	τ_{exp}	$\tau_{exp} = R_{exp} C_{RS}$
	Expiratory Flow (L/s)	$\dot{V}_E$	$\dot{V}_E = -\frac{\Delta P_e}{R_{exp}}\left(e^{-\frac{t}{\tau_e}}\right)$
	Insp. Resistance (cmH_2O/L/s)	R_{insp}	$R_{insp} = \frac{\Delta P_i}{\Delta \dot{V}}$
	Exp. Resistance (cmH_2O/L/s)	R_{exp}	$R_{exp} = \frac{\Delta P_e}{\Delta \dot{V}}$
	Compliance (L/cmH_2O)	C_{RS}	$C_{RS} = \frac{\Delta V}{\Delta P}$
	Elastance (cmH_2O/L)	E_{RS}	$E_{RS} = \frac{1}{C_{RS}}$
	Mean Airway Pressure (cmH_2O)	$\overline{P}_{aw}$	$\overline{P}_{aw} = k(PIP - PEEP)\left(\frac{T_i}{T_i + T_e}\right) - PEEP$
Primary Variable	Pressure (cmH_2O)	P	
	Volume (L)	V	
	Flow (L/s)	$\dot{V}$	
	Inspiratory Time (s)	T_i	
	Expiratory Time (s)	T_e	
	Respiratory Rate (breaths/min)	RR	

3. Operating Principles of Mechanical Ventilators for ICUs

A mechanical ventilator for intensive care units is an automatic machine designed to provide all or part of the work the body must perform to move gas into and out of the lungs [11]. Generally, it consists of two blocks:

- A pneumatic unit (internal circuit), connected to the patient's lungs through tubes (patient circuit);
- An electronic unit (microprocessor), which performs the logic operations of the pneumatic unit and measures the quantities of interest, through flow, and pressure sensors, in order to achieve the set conditions. In addition, it provides external alarms.

The key components of this sophisticated electronic machine are shown in Figure 11.

The control and setting system is considered the ventilator's brain [5]. It consists of a control panel (analogue or digital) and a microprocessor. The doctor/clinician can set the ventilation mode on the control panel, and therefore the independent variables, while also monitoring the evolution of the treatment through the waveforms of flow rate, tidal volume, and pressure. The second unit, the microprocessor, integrates data obtained from the patient with the set parameters on the ventilator. In addition, it interacts with the power, safety, and distribution systems by sending them commands and receiving data. Moreover, it allows the patient's respiratory cycle to be synchronised with the action of the machine through the opening and closing of the inspiratory and expiratory valves [8].

The power system, the heart of the ventilator [5], prepares the gas to be used for ventilating the patient. Mechanical ventilators are typically powered by electricity or pneumatic energy. Electricity, either from wall outlets (e.g., 100 to 240 AC volts at 50/60 Hz) or from batteries (e.g., 10 to 30 DC volts), is used to drive an electric motor that in turn runs

compressors of various types [7]. The energy needed to expand the patient's lungs can alternatively be supplied by compressed gas from the wall outlets of the hospital (general range 2.5–7 bar). The electric power system has the advantage of being able to be used wherever there is an electrical source; however, as the electric motor consists of bearings and connecting rods in motion, it becomes unreliable if used for a prolonged period of time [11].

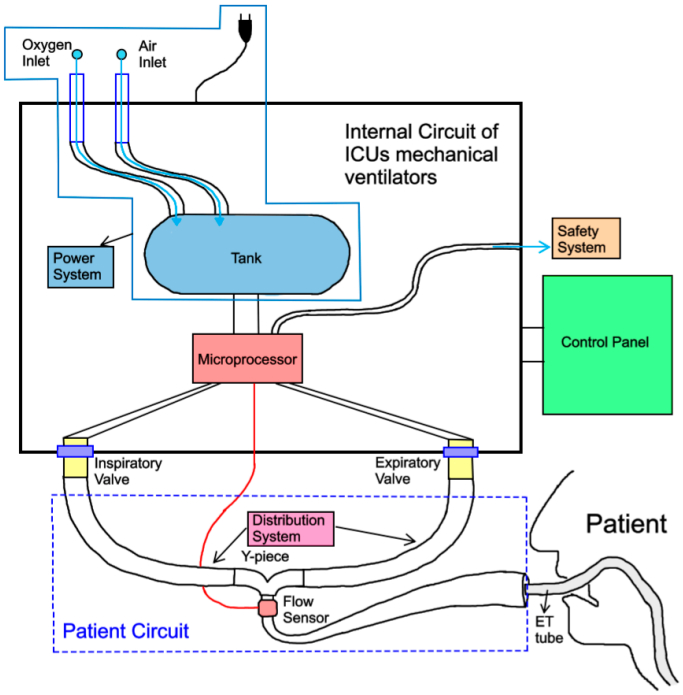

Figure 11. Key components of ICU mechanical ventilators.

The distribution system, which consists of the patient circuit and the inspiratory and expiratory valves, allows the gas received by the power system to be conveyed from/to the patient's lungs. In addition to this purely mechanical function, it also performs the task of monitoring the development of ventilation by detecting the pressure and flow rate during respiration and reporting this to the control and setting system. Furthermore, after endotracheal intubation, the upper airway loses its capacity to heat and moisture inhaled gas, hence a humidifier is introduced into the distribution system [47].

Finally, the safety system is the part of the ventilator that ensures that there are no risk situations during ventilation for the patient by indicating them to the operator [7].

The pneumatic scheme, at the base of the Simulink code, is similar to that employed by the Galileo [12] and Dräger Infinity V500 [13] intensive care ventilators, and is shown in Figure 12.

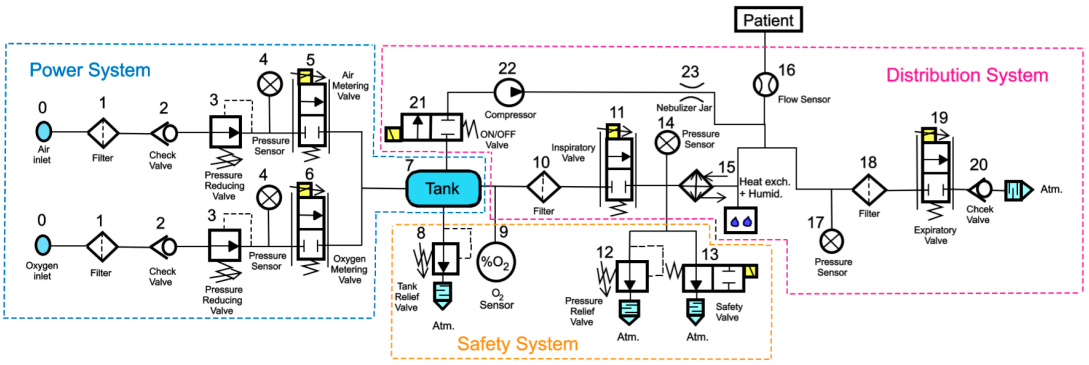

Figure 12. Pneumatic scheme of a typical ventilator for ICUs with ISO symbols.

The power system is thus made up of:

- The gas inlet connections (0), which allow the gases (oxygen and air) to enter the ventilator. These will initially follow parallel paths;
- A filter (1), used to remove impurities from incoming gases;
- A check valve (2), needed to prevent the gases from returning to the supply line;
- A pressure reducing valve (3), which allows the gas to decrease its pressure to a value of approximately 510 cmH_2O;
- A pressure sensor (4), used to measure the pressure at this point of the circuit;
- Two proportional valves, namely an air metering valve (5) and an oxygen metering valve (6), whose opening degrees can be precisely adjusted by acting on control signal(s) sent to the solenoids, allowing the system to obtain the required mixture of gas with the selected percentage of oxygen;
- A tank (7) with a large volume (approximately 5.8 L), needed for ensuring the mixture of air and oxygen is uniform, as shown in the Galileo model [12], to supply high peak flows when required, and to smooth the pressure variation at this point of the circuit (maintained within the range of 204 to 357 cmH_2O).

The safety system is thus made up of:

- A tank relief valve (8), needed to avoid uncontrolled pressure increases in the tank (7); in particular, when the pressure in the tank reaches a pre-set maximum value, the valve automatically opens and discharges the gas into the room in which the ventilator is located;
- An oxygen sensor (9), used to control the opening degree of the inlet metering valves (5) and (6), and thus to allow the system to control the oxygen concentration in the tank (7);
- A pressure relief valve (12), used in order to avoid uncontrolled pressure increases, which could harm the patients' lungs; in particular, when a pre-set maximum value for pressure is reached (namely, the cracking pressure), this valve automatically opens and discharges the gas into the external environment;
- A safety valve (13), which allows the patient to breathe in case of standby or malfunctioning of the system; during normal operation of the ventilator, both the valves (12 and 13) remain closed.

The distribution system is thus made up of:

- An additional filter (10), used to protect the downstream inspiratory valve (11) and the patient against possible contaminating particles carried by the gas;
- An inspiratory valve (11), which in the modern ventilator is a proportional valve, whose opening degree can be controlled accurately and that allows the system to obtain a precise control of the gas inhaled by the patient; in some models, such as the Galileo model [12], this valve is also equipped with a position sensor coupled with a differential pressure sensor measuring the pressure difference across the orifice of the inspiratory valve in order to calculate the flow of gas;
- A pressure sensor (14), used to measure the pressure at this point of the circuit;
- A humidification device and a heat exchanger (15) can optionally be used to control the humidity and temperature of the gas inhaled by the patient;
- A flow sensor (16), positioned close to the patient's mouth, in order to measure and monitor the flow of gas inhaled and exhaled by the patient;
- A pressure sensor (14), used to measure the pressure at this point of the circuit;
- An optional additional filter (18);
- An expiratory valve (19), a proportional valve used both to adjust the minimum pressure in the patient circuit and to regulate the flow of expiratory gases from the patient to the external environment;
- A check valve (20), used to avoid reverse flow in the expiratory circuit.

Components relating to the nebulizer can be added to the above components when it is necessary to administer medicines to the patient in the form of aerosols. The operation of

the nebulizer controls the opening of the ON/OFF directional valve (21) and the compression of the gas taken from the tank through a mini-compressor (22) until the gas reaches approximately 918 cmH_2O. Finally, the gas enters a nebulizer vessel (23) to mix with the medicine to be supplied to the patient.

In order to tackle the COVID-19 pandemic, the MHRA has recently established some guidelines concerning the operating parameters of the ventilator that must be achieved [16]. These include:

- Plateau pressure (P_{plt}) should be adjusted to achieve volume and must be limited to 35 cmH_2O by default;
- If VC-CMV is used, the operator/clinician must be able to set the inspiratory airway pressure limit in the range of at least 15–40 cmH_2O in at least 5 cmH_2O increments;
- The mechanical failsafe valve (see pressure relief valve (12)) must open itself at 80 cmH_2O;
- Peak pressure (PIP) should be no more than 2 cmH_2O greater than plateau pressure;
- The patient breathing system must remain pressurised to at least the PEEP level setting at all times;
- The positive end-expiratory pressure (PEEP) must be greater than 5 cmH_2O, adjustable in at least 5 cmH_2O increments.

4. Simulation Code VC-CMV Mode

A simulation code, reproducing the pneumatic scheme of Figure 11, has been produced in Simulink, software developed by MathWorks® based in Natick, MA, USA. In particular the Simscape Fluids (gas) library [39,40] has been used. The code, whose graphical scheme is shown in Figure 13, can easily be reproduced and used by manufacturers, and is available at the link provided in [48].

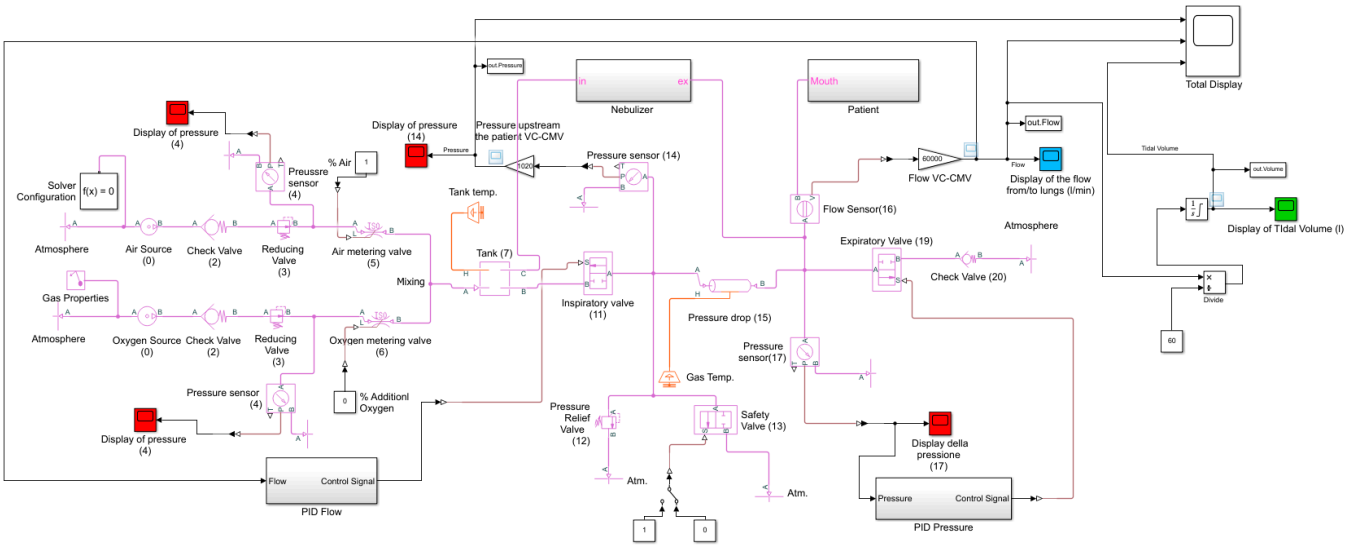

Figure 13. VC-CMV simulation code produced with Simulink (Simscape Fluids (gas) library).

In particular, it consists of:

- The "Gas Properties" block, which allows the user to select from three gas propriety models: perfect gas, semi-perfect gas, or real gas; the specific gas constant is also set in this block;
- The "Pressure Source" block, used to simulate the air and oxygen sources (0); this block maintains a constant pressure at its outlet;
- The "Check Valve" block, which reproduces the check valves (2 and 20) and allows the flow to go in only one direction; the cracking pressure, which is the minimum upstream pressure required to open the valve, is set in this block;

- The "Reducing Valve" block, used to simulate the pressure reducing valve (3); the valve remains open when the downstream pressure is less than the set pressure, defined in the block proprieties;
- The "Pressure and Temperature Sensor" block, which reproduces the pressure sensors (4, 14, and 17) in order to monitor the pressure downstream of the pressure reducing valves, and downstream of the inspiratory and expiratory valves;
- The "Variable Orifice ISO 6358" block, used to simulate the air and oxygen metering valves (5 and 6); this block models a controlled pressure loss from port A to port B, based on the ISO 6358 standard, which can represent a valve, orifice, or restriction. The orifice opening fraction between 0 (valve closed) and 1 (maximum opening) is set by the control signal at port L. The valve properties, inside the block, can be set using the sonic conductance, the flow coefficient, or the restriction area of the corresponding valve;
- The "Constant Volume Chamber" block, used to reproduce the tank (7); the tank volume, located inside the block, can be set. The pressure in the tank is calculated according to the mass, the volume, and the temperature of the tank. This block is characterised by four ports: a sole inlet port (port A), two outlet ports (port B, connected to the downstream inspiratory valve (11), and port C, connected to the nebulizer), and the thermal conserving port associated with the thermal mass of the gas volume (port H);
- The "Two-Way Directional Valve" block, used to simulate the inspiratory and expiratory valve (11 and 19); the flow rate is calculated according to the ISO 6358 standard. The gas flows from port A to port B, and the open connection between these gas ports is determined by a positive control signal at port S. The valve properties can be set in the block using the sonic conductance, the flow coefficient, or the restriction area of the corresponding valve;
- The "Pressure Relief Valve" block, which reproduces the pressure relief valve (12); during normal operation the valve remains closed; however, if the upstream pressure is higher than the maximum pressure set in the block, the valve opens to permit gas flow;
- The "Two-Way Directional Valve" block, used to simulate the safety valve (13); during normal operation the valve is closed (the control signal is 0 at port S); however, if the system malfunctions, it opens to allow the patient to breathe out (the control signal is 1 at port S);
- The "Pipe" block, implemented in order to take into account the pressure drops in the circuit due to the presence of the heat exchanger and humidifier (15); this is possible by setting an equivalent length and an equivalent diameter in the block;
- The "Volumetric Flow Rate Sensor" block, which reproduces the flow sensor (16) in order to measure the flow rate (and tidal volume) inspired (>0) and expired (<0) by the patient.

The patient is simulated using the subroutine "Patient" shown in Figure 14.
It consists of:

- Two "Check Valve" blocks, used to allow the gas to flow through the upper/lower branch during inspiration/expiration, respectively; the cracking pressure, which is the minimum upstream pressure required to open the valve, is set in these blocks;
- Two "Local Restriction" blocks, which reproduce the inspiratory/expiratory resistance of the respiratory system, respectively; these blocks model the pressure loss due to a flow area restriction, the value of which can be set inside the blocks. The laminar flow pressure ratio and the cross-sectional area at the inlet/outlet port must also be defined in order to consider the type of flow conditions in the trachea and its dimensions;
- The "Translational Mechanical Converter" block (namely, a piston moving inside a cylinder), used to simulate the patient's lungs (12);
- The "Spring" block, connected in series with the "Translational Mechanical Converter" block and used to simulate the compliance of the respiratory system.

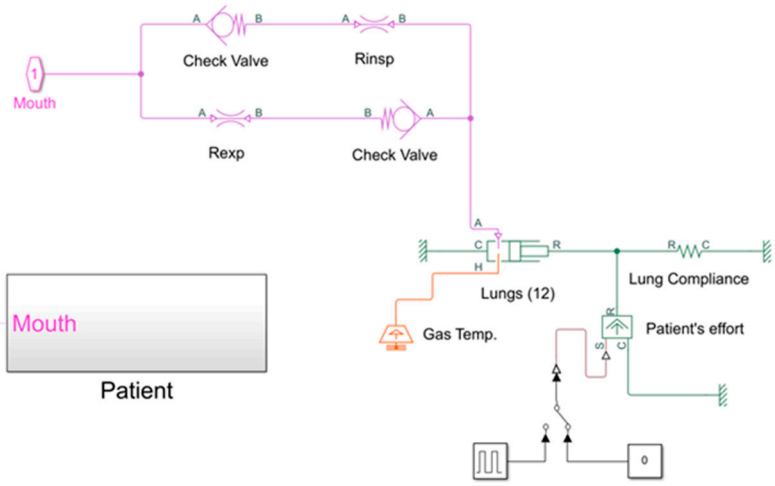

Figure 14. Subroutine reproducing the patient's trachea and lungs.

The piston diameter and the spring stiffness must be chosen according to the compliance of the respiratory system of the simulated patient. The compliance of the respiratory system (C_{RS}) is defined as the change in volume of the lungs (ΔV) that occurs per unit change in the pressure inside the lungs (ΔP):

$$C_{RS} = \frac{\Delta V}{\Delta P}, \tag{16}$$

As the lungs are simulated in the same way as a cylinder whose piston is counteracted by a spring, the relation between (ΔP) and (ΔV) is:

$$\Delta P = \frac{k\Delta x}{A} = \frac{k\Delta V}{A^2}, \tag{17}$$

where (A) is the piston area, (Δx) is the displacement of the piston, and (k) is the stiffness of the spring. Combining Equations (16) and (17), one obtains:

$$C_{RS} = \frac{A^2}{k}, \tag{18}$$

Equation (18) allows us to calculate (k) once (A) has been fixed (or vice versa) by establishing the value of the simulated patient compliance. Furthermore, once we have established the value of the minimum pressure that we want in the circuit at the beginning of the inspiratory phase, namely the positive end-expiratory pressure (PEEP), the pre-compression of the spring (x_0) can be evaluated as follows:

$$x_0 = \frac{A}{k} PEEP, \tag{19}$$

Finally, the following equation (Equation (20)) allows the dead volume of the cylinder (V_0) to be calculated:

$$V_0 = A\, x_0, \tag{20}$$

For contrast, the subroutine reproducing the nebulizer is shown in Figure 15.

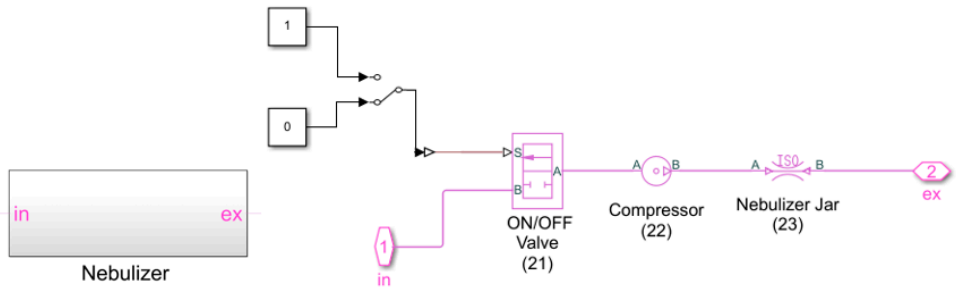

Figure 15. Subroutine reproducing the nebulizer.

It consists of:

- The "Two-Way Directional Valve" block, used to simulate the ON/OFF valve (21); the control signal, at port S, being equal to either 0 or 1;
- The "Pressure Source" block, which reproduces the compressor (22); this block maintains a constant pressure at its outlet and its value can be set inside the block;
- The "Orifice ISO 6358" block, used to reproduce the nebulizer jar (23); again, the valve properties inside the block can be set using the sonic conductance, the flow coefficient, or the restriction area of the corresponding valve.

The automatic control of the inspiratory flow and the positive end-expiratory pressure, which is therefore the automatic control of the opening degrees of the inspiratory and expiratory valves, has been obtained through two proportional-integral-derivative (PID) controllers: "PID Flow" and "PID Pressure". The parameters of the PID controllers have been determined using the Ziegler–Nichols method. The subroutines reproducing these controllers are shown in Figures 16 and 17, respectively.

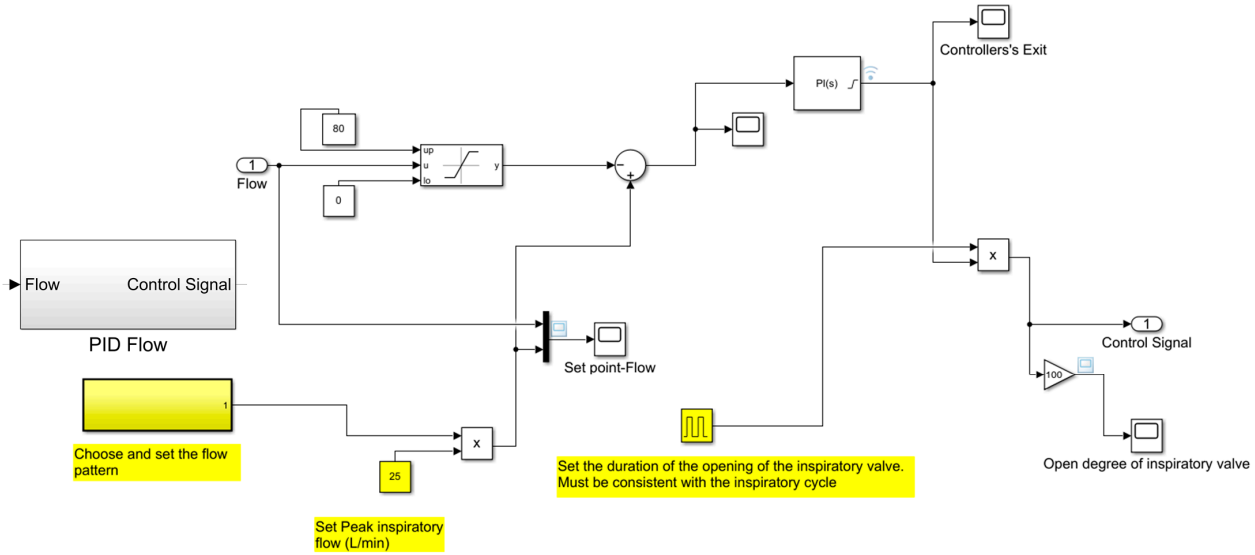

Figure 16. Subroutine reproducing the automatic control of the inspiratory flow.

The resulting set of ordinary differential equations describing the dynamics of the system with respect to time are solved by the solver Ode 23t with variable time steps (from 0.001 to 0.1 s) [39,40].

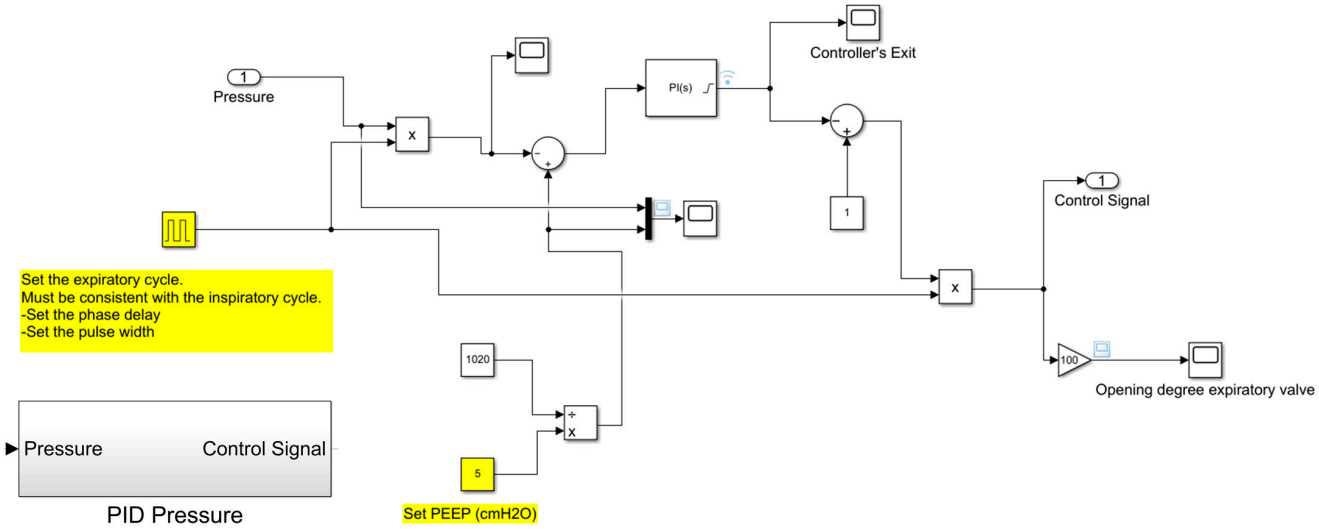

Figure 17. Subroutine reproducing the automatic control of the positive end-expiratory pressure.

5. Simulation Code PC-CMV Mode

The simulation code, shown in Figure 18, was made again using the Simscape Fluids (gas) library of MathWorks® Simulink [39,40]. The only difference from the previous simulation code (VC-CMV mode) is that, in this case, the automatic control of the opening degree of the inspiratory valve during the cycle has been obtained through the control of the inspiratory pressure. Indeed, in PC-CMV mode, the inspiratory flow is a consequence of the ventilator's attempt to maintain a pre-set pressure waveform.

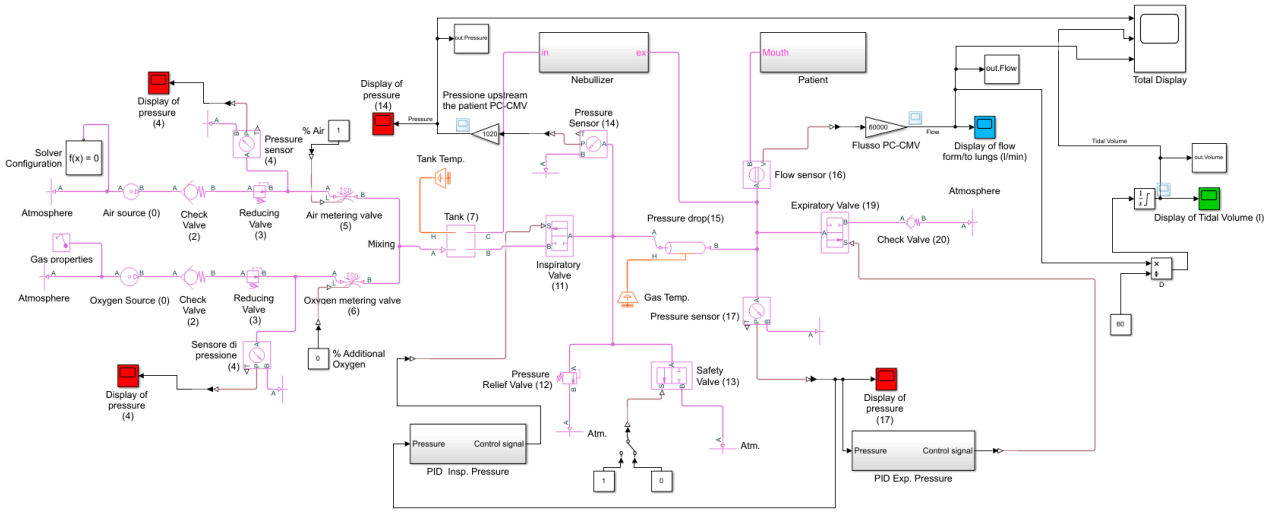

Figure 18. PC-CMV simulation code produced with Simulink (Simscape Fluids (gas) library).

The subroutine reproducing the automatic control of the inspiratory pressure is shown in Figure 19.

The resulting set of ordinary differential equations describing the dynamics of the system with respect to time are solved by the solver Ode 23t with variable time steps (from 0.001 to 0.1 s) [39,40].

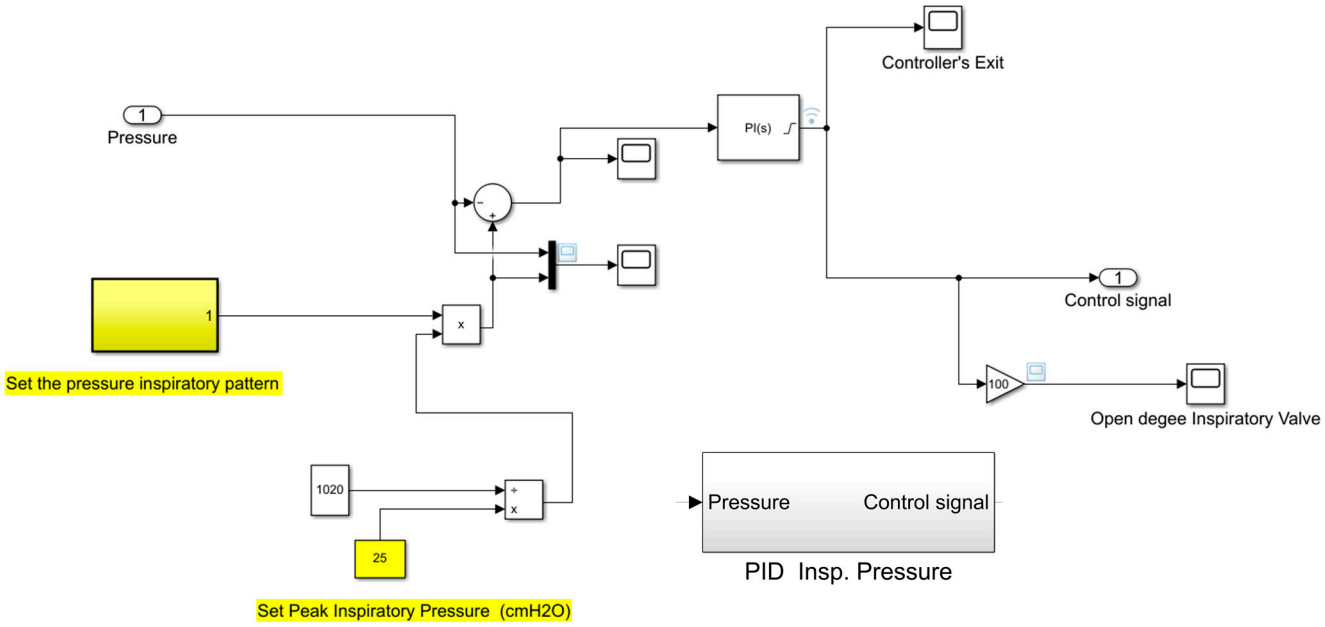

Figure 19. Subroutine reproducing the automatic control of the inspiratory pressure.

6. Simulation Code Airway Resistance

A fundamental aspect to consider in order to validate the results provided by the simulation codes relates to the incidence of pressure losses that are generated in the respiratory system and, particularly in the trachea, where the greatest losses occur. For this reason, we need to calculate the resistance that the respiratory system offers to the passage of the gas flow. This is useful to simulate several patients who each have a different structure of the respiratory epithelium and, consequently, a different resistance value to consider.

Therefore, an additional simulation code is needed with a view to determining the resistance of the respiratory system. In particular, its value is related to the value of the restriction area that has to be set in the "Local Restriction" block located in the subroutine "Patient".

Again, the simulation code concerning the airway resistance was created in MathWorks® Simulink using the Simscape Fluids (gas) library [39,40], and is shown in Appendix A.

The gas mixture that arrives in the patient's mouth has been simulated using the "Pressure Source" block (1). This block, which maintains a constant pressure equal to 306 cmH_2O at its outlet, is directly connected to the "Local Restriction block" (2), which is then used to reproduce the resistance of the respiratory system. Inside this block the following parameters have to be set:

- The value of restriction area, so that different resistance values of the respiratory system can be evaluated;
- The "laminar flow pressure ratio", a dimensionless coefficient set equal to 0.01 in order to indicate the fully developed laminar flow conditions inside the trachea;
- The value of the cross-sectional area at the inlet/outlet port, calculated according to the size of the diameter of the patient's trachea (in the simulation code an average diameter of 25 mm has been considered, obtaining a section equal to 5×10^{-4} m^2);

Two "Pressure and Temperature Sensor" blocks (3 and 4) have been positioned upstream and downstream of the "Local Restriction" block in order to measure the pressure losses in the trachea. Similarly, the "Volumetric Flow Rate Sensor" block (5) has been placed downstream of the "Local Restriction" block in order to measure the flow rate that arrives at the patient's lungs. The key of the simulative model is performed by the "Product" block (6); the pressure losses recorded by the two pressure sensors are divided by the flow rate and recorded by the flow sensor, resulting in a precise airway resistance value.

The method adopted to evaluate the value of the resistance of the respiratory system facilitates the iteration of restriction area values to be inserted into the "Local Restriction" block in order to select the restriction area value that allows us to obtain the desired resistance value. For instance, a resistance of respiratory system equal to 10 $cmH_2O/L/s$ is obtained by setting inside the "Local Restriction" block a restriction area value equal to 2.328×10^{-4} m^2, while a restriction area equal to 1.466×10^{-4} m^2 has to be set in order to have a resistance of the respiratory system equal to 20 $cmH_2O/L/s$, as shown in Appendix A.

7. Validations

Using the numerical codes described in Sections 4–6, the respiratory cycle can be simulated for different control strategies (i.e., volume- or pressure-controlled), for different patients' characteristics (i.e., compliance and inspiratory/expiratory resistance of the respiratory system), and for different geometric characteristics (i.e., valve size and tank size) and operating parameters (i.e., pressures, flow rates, and tidal volumes) of the ventilator. In this way, several scenarios can be predicted.

In this section, the simulation results of both modes in terms of pressure, flow, and tidal volume are compared with trends derived from real-life quantitative data [46,49] and previously recorded real-life experiments [43], in order to validate the previous Simulink models. Thus, three different cases are simulated. The real-life trends of Case 1 and Case 2 are shown in Figures 20 and 21, respectively.

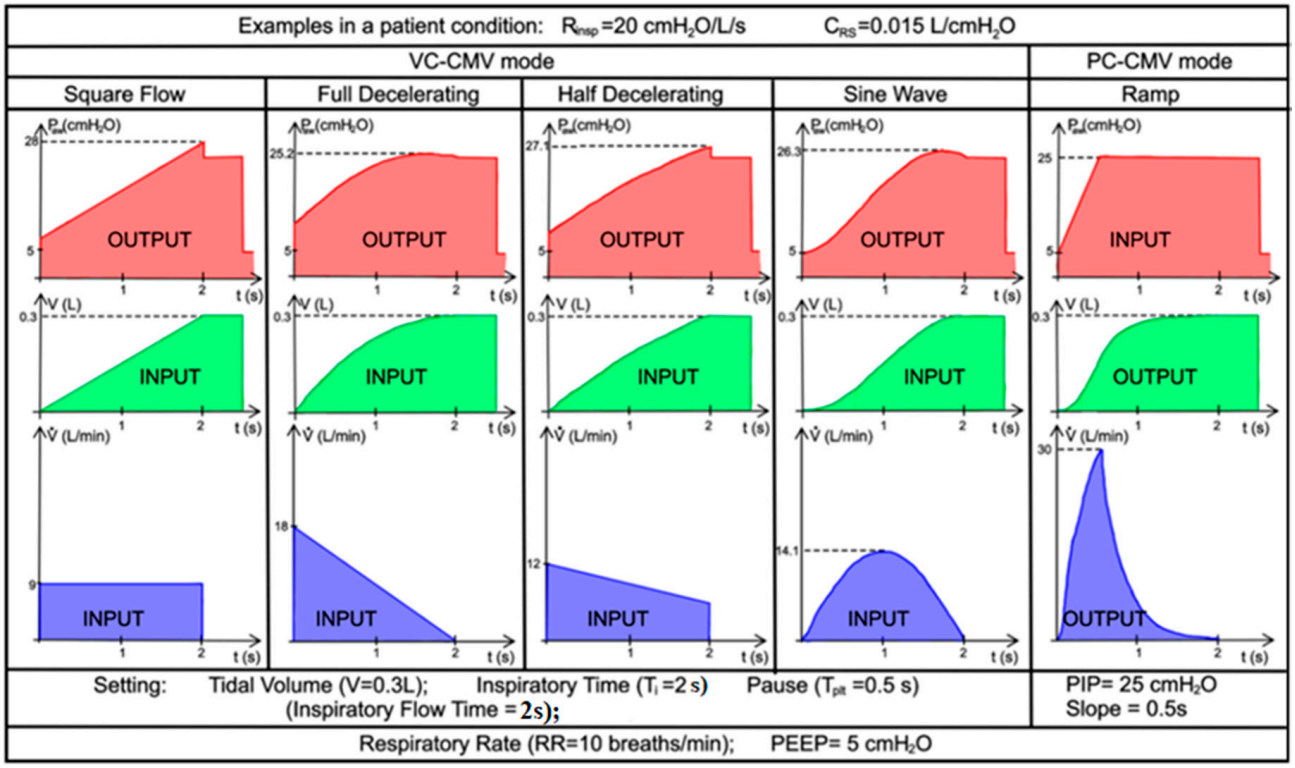

Figure 20. Case 1. Real-life quantitative data of flow, volume, and pressure waveforms on various patterns of inspiratory flow, adapted from [46].

The patient's respiratory effort is zero, so the lung ventilator performs 100% of the respiratory work; inspiration and expiration are regulated by the ventilator itself. The operating and geometrical parameters of the ventilator used in the simulations are shown in Table 4.

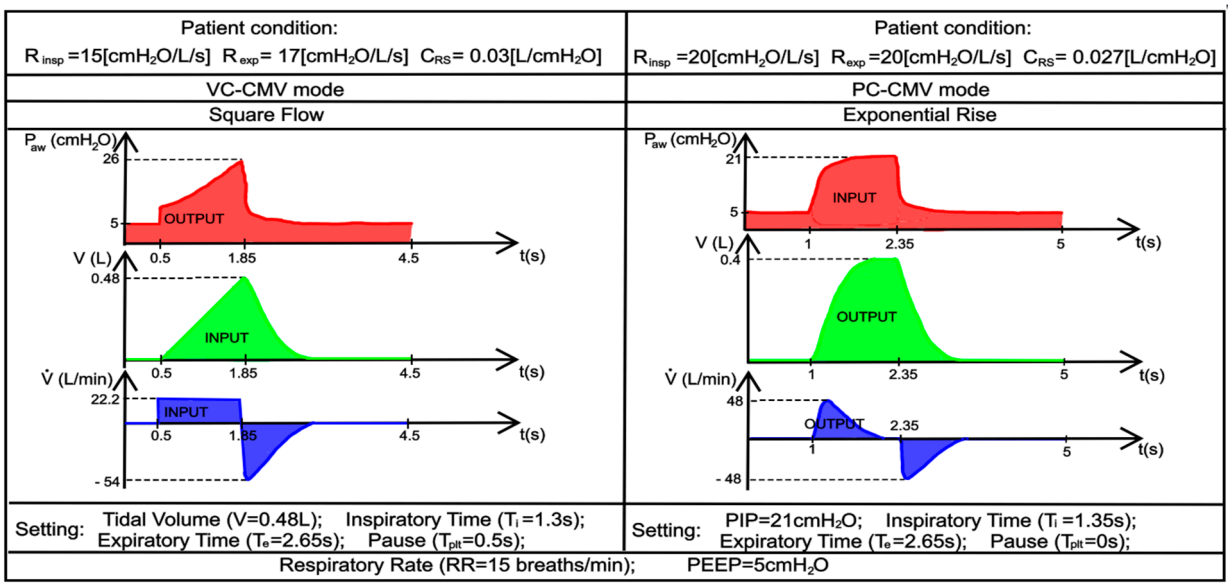

Figure 21. Case 2. Recorded real-life trends of flow, volume, and pressure waveforms in VC-CMV and PC-CMV mode, adapted from [43].

On the other hand, the independent, dependent, and patient variables of the simulated patient are provided by the real-life trends presented in Figures 20 and 21, and are shown in Tables 5 and 6, respectively. The equations concerning volume- and pressure-controlled modes, presented in Section 2.2 (Table 3), were used in order to obtain these variables.

Table 4. Operating and geometrical parameters of the ventilator.

Parameter	Value
Control mode	VC-CMV/PC-CMV
Trigger mode	Ventilator
O_2 percentage in the gas	20.9%
Nebulizer	Not activated
Specific gas constant	287.1 J/kg K
Critical pressure ratio	0.53
Supply pressure	2039.4 cmH_2O
Pressure downstream of the pressure reducing valve	306 cmH_2O
Cracking pressure of the pressure relief valve	80.0 cmH_2O
Cracking pressure of the check valves	1.02 cmH_2O
Sonic conductance at maximum flow for the air metering valve, oxygen metering valve, inspiratory valve, and expiratory valve	10 L/s/bar
Opening offset of the inspiratory and expiratory valves	−10%
Tank volume	6 L
Temperature in the tank	20 °C
Pressure drop heat exchanger + humidifier (Equivalent length and diameter)	I0.5 m × 0.01 m
Temperature gas heat exchanger	27 °C

Table 5. Independent, dependent, and patient variables of the real-life trends of the Case 1.

VC-CMV mode														
	Independent Variables					Patient Variables			Dependent Variables					
	V_T (L)	I_{pf} (L/min)	T_i (s)	RR (breaths/min)	PEEP (cmH_2O)	R_{insp} (cmH_2O/L/s)	C_{RS} (L/cmH_2O)	τ_i (s)	PIP (cmH_2O)	P_{plt} (cmH_2O)	T_{plt} (s)	T_e (s)	TCT (s)	
Square Flow	0.3	9	2	10	5	20	0.015	0.3	28	25	0.5	3.5	6	
Half Decelerating	0.3	12	2	10	5	20	0.015	0.3	27.1	25	0.5	3.5	6	
Full Decelerating	0.3	18	2	10	5	20	0.015	0.3	25.2	25	0.5	3.5	6	
Sinus Waveform	0.3	14.14	2	10	5	20	0.015	0.3	26.3	25	0.5	3.5	6	
PC-CMV mode														
	Independent Variables					Patient Variables				Dependent Variables				
	PIP (cmH_2O)	Slope (s)	T_i (s)	RR (breaths/min)	PEEP (cmH_2O)	R_{insp} (cmH_2O/L/s)	C_{RS} (L/cmH_2O)	ΔP (cmH_2O)	τ_i (s)	V_T (L)	I_{pf} (L/min)	T_{plt} (s)	T_e (s)	TCT (s)
Ramp	25	0.5	2	10	5	20	0.015	20	0.3	0.3	30	0.5	3.5	6

Table 6. Independent, dependent and patient variables of the real-life trends of the Case 2.

VC-CMV															
Square Flow															
Independent Variables					Patient Variables					Dependent Variables					
V_T (L)	I_{pf} (L/min)	T_i (s)	RR (breaths/min)	PEEP (cmH_2O)	R_{insp} (cmH_2O/L/s)	R_{exp} (cmH_2O/L/s)	C_{RS} (L/cmH_2O)	τ_i (s)	τ_e (s)	PIP (cmH_2O)	P_{plt} (cmH_2O)	E_{pf} (L/min)	T_{pltl} (s)	T_e (s)	TCT (s)
0.48	22.2	1.3	15	5	15	17	0.03	0.45	0.51	26	20.5	−54	0.05	2.65	4
PC-CMV mode															
Square Pressure															
Independent Variables				Patient Variables					Dependent Variables						
PIP (cmH_2O)	T_i (s)	RR (breaths/min)	PEEP (cmH_2O)	R_{insp} (cmH_2O/L/s)	R_{exp} (cmH_2O/L/s)	C_{RS} (L/cmH_2O)	ΔP (cmH_2O)	τ_i/τ_e (s)	V_T (L)	I_{pf}/E_{pf} (L/min)	T_{plt} (s)	T_e (s)	TCT (s)		
21	1.35	15	5	20	20	0.027	16	0.54	0.4	±48	0	2.65	4		

Tables 7 and 8 reveal the parameters entered into the subroutine "Patient" to obtain the values of compliance and the inspiratory/expiratory resistance of the respiratory system. The airway resistance simulation code, which is shown in Appendix A, and the equations, presented in Section 4, have been used for this propose.

Table 7. Parameters set in the subroutine "Patient" concerning simulations of real-life cases of the Case 1.

		Parameters				
		Piston Area (A) m^2	**Spring Stiffness (k) N/m**	**Spring Pre-Compression (x_0) m**	**Cylinder Dead Volume(V_0) L**	**Restriction Area to Simulate the Inspiratory Resistance ($A_{r,i}$) m^2**
VC-CMV	Square Flow	0.01	653	0.0077	0.077	0.0001466
	Half Decel.	0.01	653	0.0077	0.077	0.0001466
	Full Decel.	0.01	653	0.0077	0.077	0.0001466
	Sinus Waveform	0.01	653	0.0077	0.077	0.0001466
PC-CMV	Ramp	0.01	653	0.0077	0.077	0.0001466

Table 8. Parameters set in the subroutine "Patient" concerning simulations of real-life cases of the Case 2.

		Parameters					
		Piston Area (A) m^2	**Spring Stiffness (k) N/m**	**Spring Pre-Compression (x_0) m**	**Cylinder Dead Volume (V_0) L**	**Restriction Area to Simulate the Inspiratory Resistance ($A_{r,i}$) m^2**	**Restriction Area to Simulate the Expiratory Resistance ($A_{r,e}$) m^2**
VC-CMV	Square Flow	0.01	326	0.0153	0.153	0.0001797	0.000165
PC-CMV	Square Pressure	0.01	359	0.0139	0.139	0.0001466	0.0001466

Once all the data have been set in the simulation codes, the simulations can be carried out. The collected data of tidal volume, flow, and pressure, shown in Appendix A, are compared with those indicated above in the real-life examples, as shown in Figures 20 and 21, respectively. In particular, in Figures 22 and 23, the predicted trends of the pressure, tidal volume, and flow rate inspired and expired by the simulated patient are compared with the corresponding real-life quantitative trends provided in the literature [43–46]. The comparison, shown in Figure 22, highlights the strong agreement between the numerical predictions and the real-life trends; the percentage error being, on average, well below 10%. The obtained values of inspiratory/expiratory flow, tidal volume, and pressure are very similar to those reported in Table 5.

Conversely, the comparison shown in Figure 23 highlights the cases where the percentage error is greater than 10%. This is essentially due to:

- In Case 2, during VC-CMV, the compliance does not remain constant during the inspiration. The compliance changes during inspiration due to the fact that the variation of the stress index, obtained by the pressure–time curve, has not been implemented into the Simulink model.
- In Case 2, during PC-CMV, an exponential rise has been used as the inspiratory pressure pattern, whereas in the Simulink model, a square pressure pattern has been employed.

The proposed simulation codes are also useful for predicting the behaviour of the valves employed in the patient circuit. In this regard, Figure 24 shows the behaviour of the inspiratory and expiratory valves during a breathing cycle, with reference to Case 2. It is shown that, as expected, the inspiratory valve is opened during the inspiratory phase, and then it is closed during the expiratory phase, ensuring that the inlet gas is not lost during the patient's expiration.

In addition to this, Figure 25 shows, again referring to Case 2, how the control system is fully effective during the simulation: the flow and pressure waveforms on which the control is carried out accurately reach the set points, pre-set by the operator, during both the VC-CMV mode and the PC-CMV mode.

Finally, the effects on inspiratory/expiratory resistance and lung compliance changes during the two previously analysed ventilation modes are evaluated in the Case 3. The considered data, shown in Figure 26, are taken from real-life quantitative experiments reported in the literature [49].

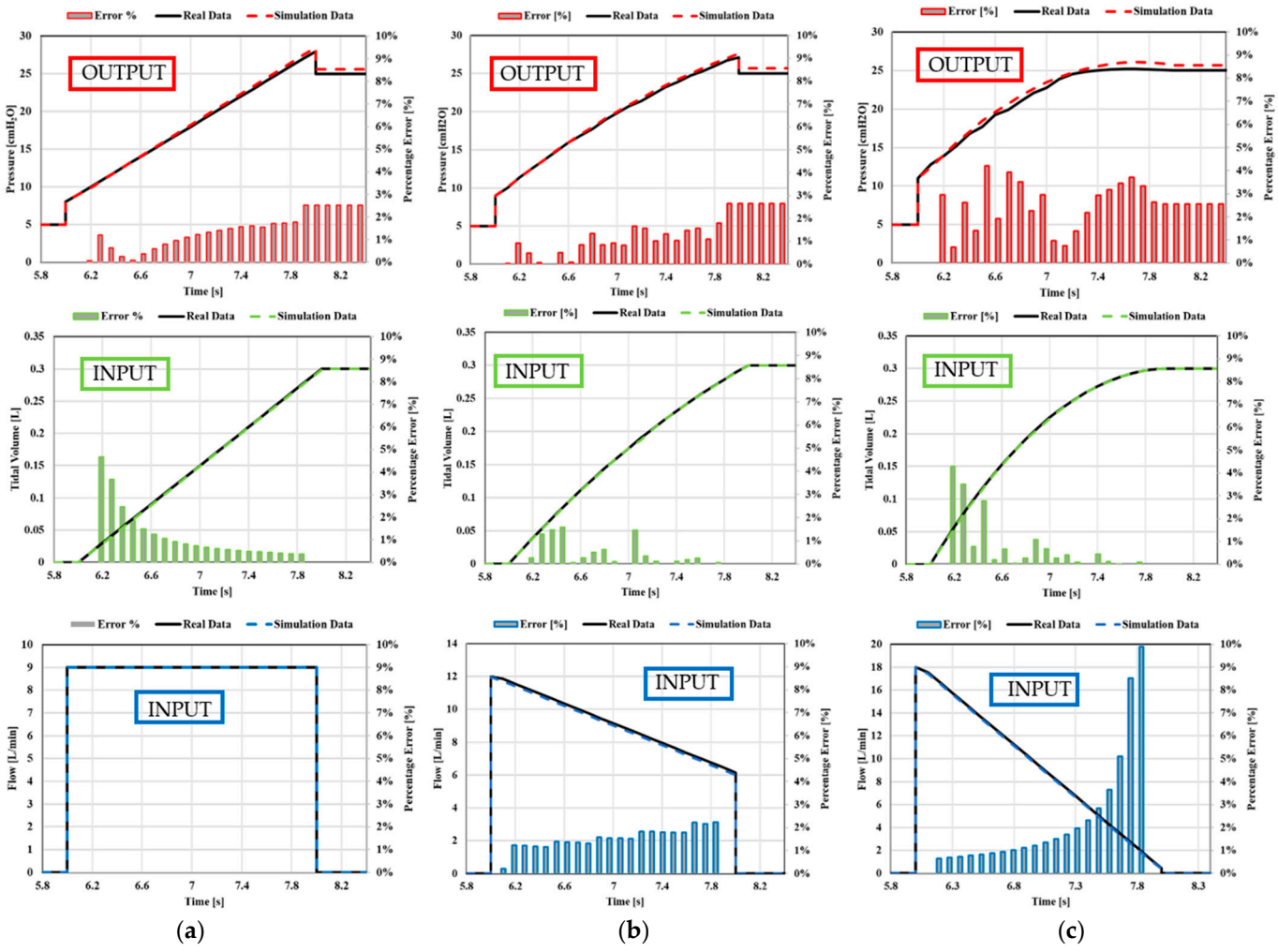

Figure 22. *Cont.*

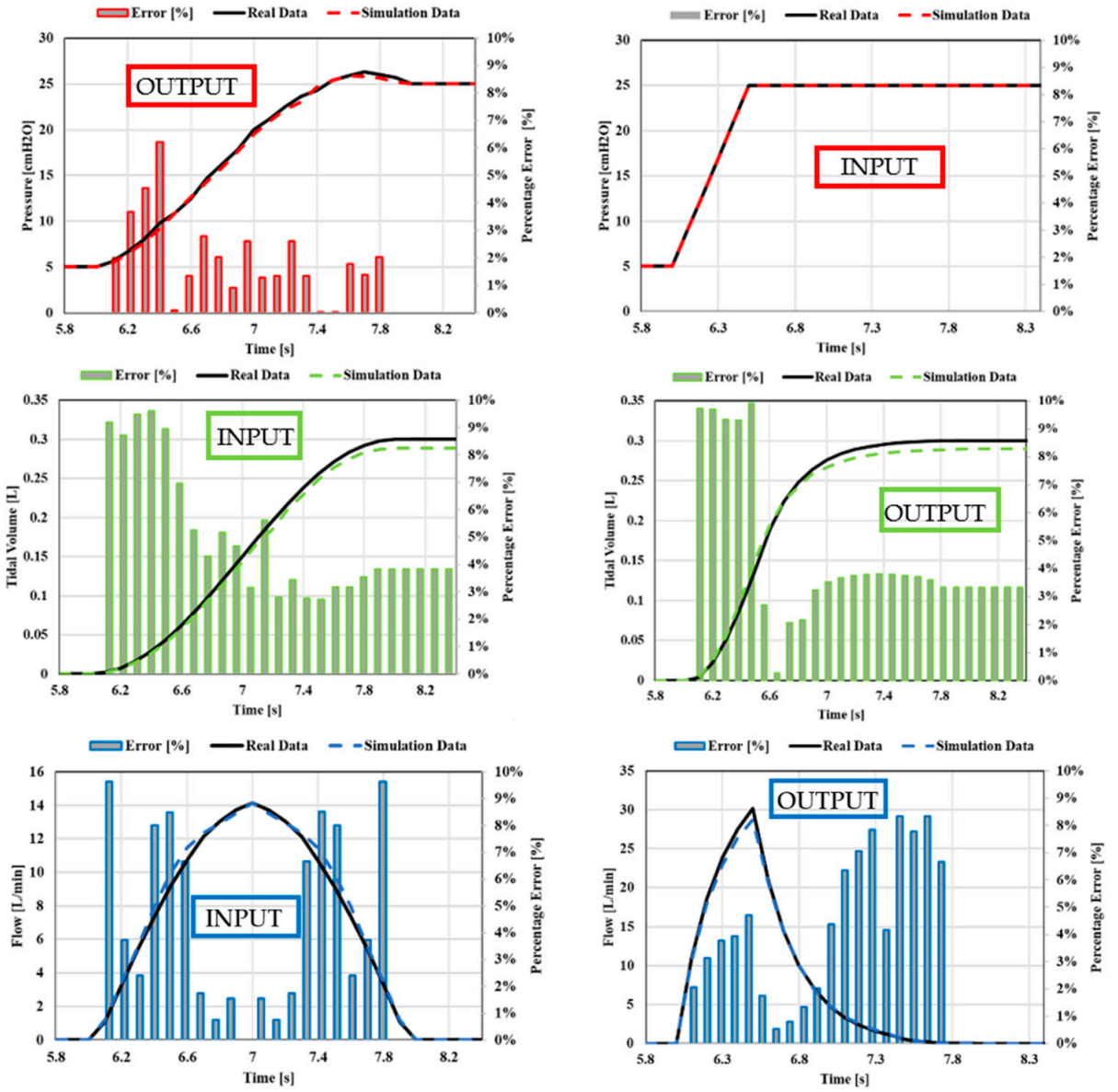

Figure 22. Case 1. Comparison between real-life data and simulation data: (**a**) square flow, (**b**) half decelerating; (**c**) full decelerating; (**d**) sine waveform; (**e**) ramp pressure.

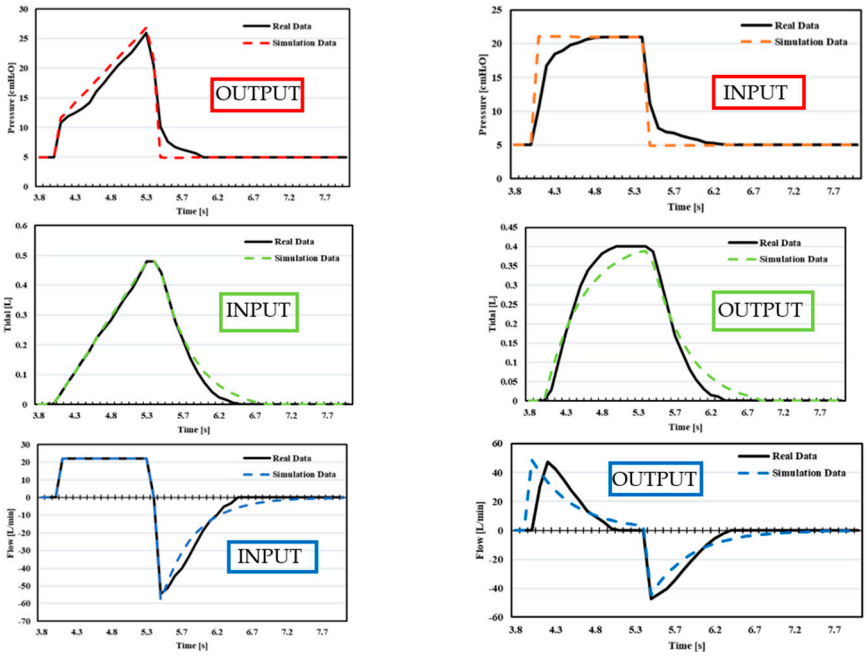

Figure 23. Case 2. Comparison between real-life data and simulation data: (**a**) VC-CMV mode, (**b**) PC-CMV mode.

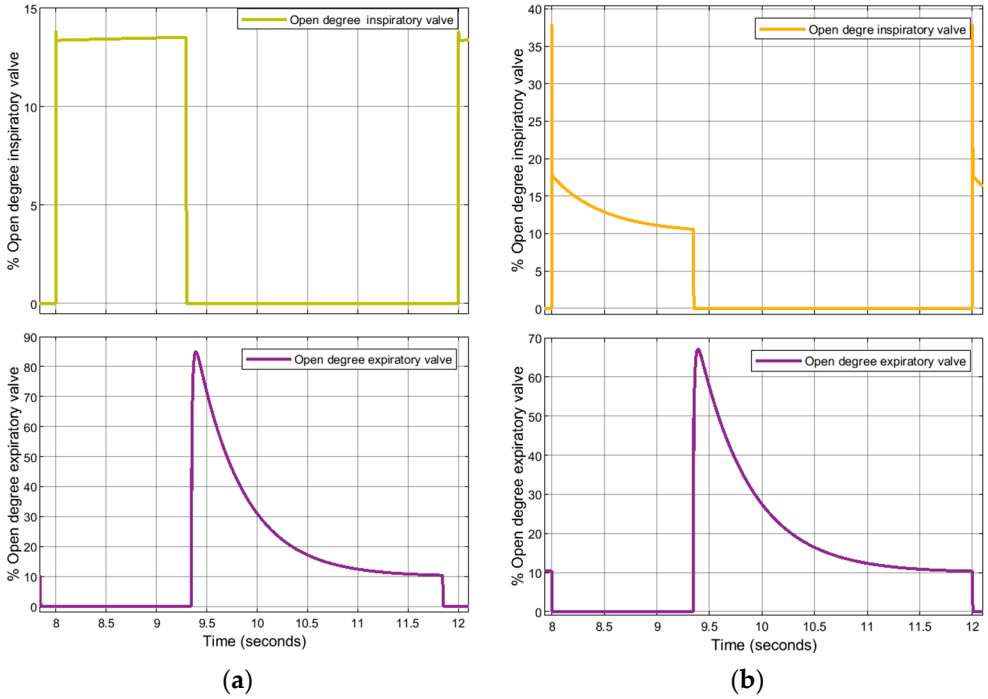

Figure 24. Case 2. Opening degree of the inspiratory and expiratory valves: (**a**) VC-CMV mode; (**b**) PC-CMV mode.

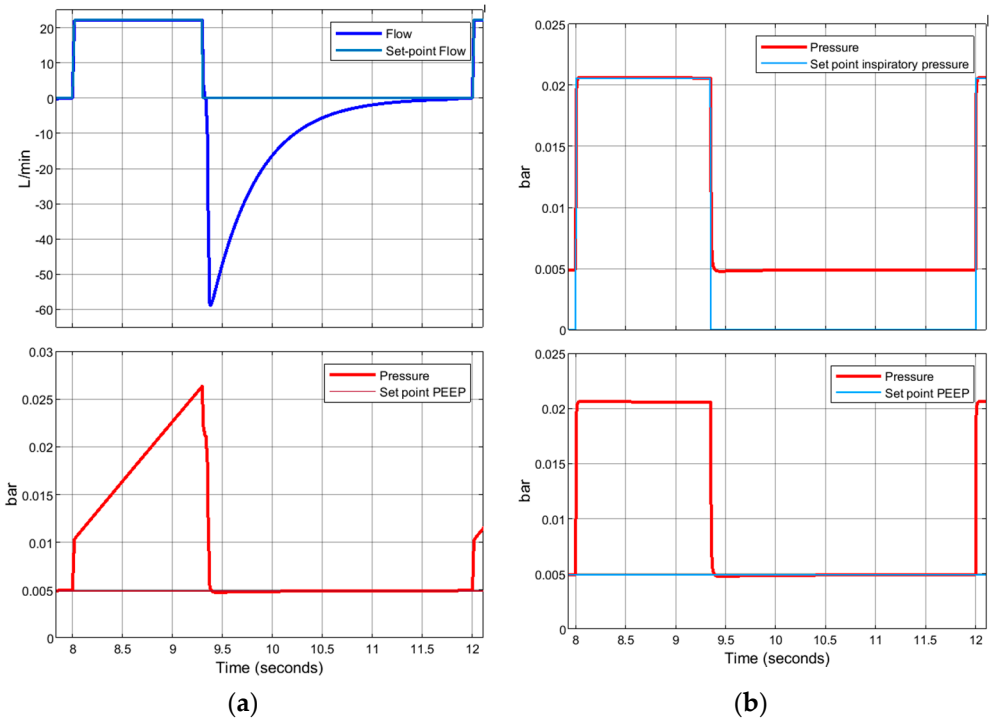

Figure 25. Case 2. Control system: (**a**) VC-CMV mode; (**b**) PC-CMV mode.

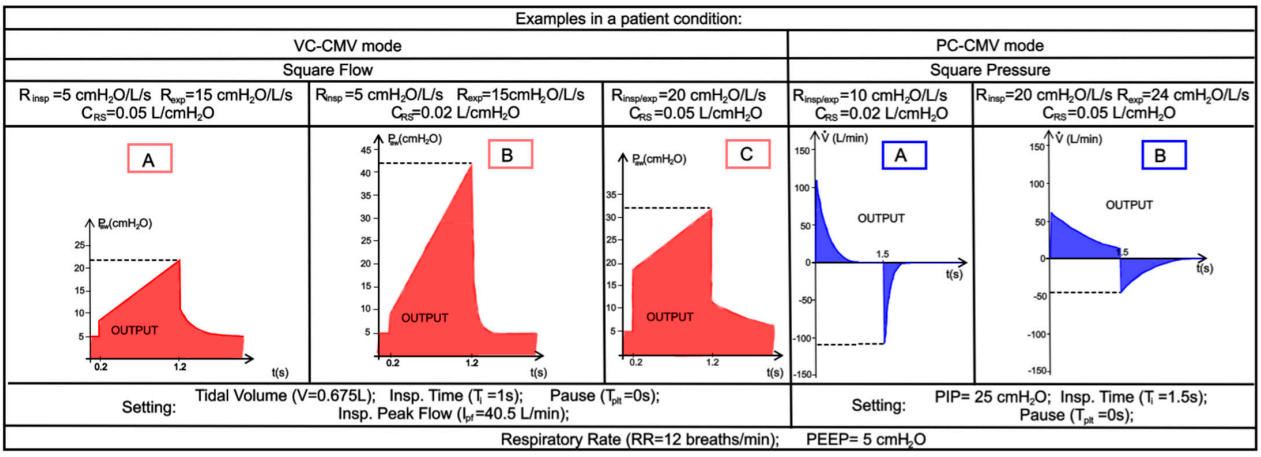

Figure 26. Case 3. Real-life trends of pressure (VC-CMV mode, in red) and flow (PC-CMV mode, in blue) concerning the inspiratory/expiratory resistance and lung compliance changes, adapted from [49]. VC-CMV mode ([A] C_{RS} = 0.05 L/cmH_2O, R_{insp} = 5 cmH_2O/L/s, R_{exp} = 15 cmH_2O/L/s; [B] C_{RS} = 0.02 L/cmH_2O, R_{insp} = 5 cmH_2O/L/s, R_{exp} = 15 cmH_2O/L/s; [C] C_{RS} = 0.05 L/cmH_2O, $R_{insp/exp}$ = 20 cmH_2O/L/s); PC-CMV mode ([A] C_{RS} = 0.02 L/cmH_2O, $R_{insp/exp}$ = 10 cmH_2O/L/s; [B] C_{RS} = 0.05 L/cmH_2O, $R_{insp/exp}$ = 20 cmH_2O/L/s).

The operating and geometrical parameters of the ventilator, shown in Table 4, are the same as those used in the previous simulations, while the independent, dependent, and patient variables are reported in Table 9.

Table 9. Independent, dependent, and patient variables of the real-life trends of the Case 3.

	VC-CMV mode															
	Square Flow															
	Independent Variables					**Patient Variables**					**Dependent Variables**					
	V_T (L)	**I_{pf} (L/min)**	**T_i (s)**	**RR (breaths/min)**	**PEEP (cmH_2O)**	**R_{insp} (cmH_2O/L/s)**	**R_{exp} (cmH_2O/L/s)**	**C_{RS} (L/cmH_2O)**	**τ_i (s)**	**τ_e (s)**	**PIP (cmH_2O)**	**P_{plt} (cmH_2O)**	**E_{pf} (L/min)**	**T_{pltl} (s)**	**T_e (s)**	**TCT (s)**
A	0.675	40.5	1	12	5	5	15	0.05	0.25	0.75	21.875	18.5	−54	0	4	5
B	0.675	40.5	1	12	5	5	15	0.02	0.1	0.3	42.125	38.75	−135	0	4	5
C	0.675	40.5	1	12	5	20	20	0.05	1	1	32	18.5	−40.5	0	4	5
	PC-CMV mode															
	Square Pressure															
	Independent Variables					**Patient Variables**					**Dependent Variables**					
	PIP (cmH_2O)	**T_i (s)**	**RR (breaths/min)**	**PEEP (cmH_2O)**	**R_{insp} (cmH_2O/L/s)**	**R_{exp} (cmH_2O/L/s)**	**C_{RS} (L/cmH_2O)**	**ΔP (cmH_2O)**	**τi (s)**	**τe (s)**	**V_T (L)**	**I_{pf} (L/min)**	**E_{pf} (L/min)**	**T_{plt} (s)**	**T_e (s)**	**TCT (s)**
A	25	1.5	12	5	10	10	0.02	20	0.2	0.2	0.4	120	−120	0	3.5	5
B	25	1.5	12	5	20	20	0.05	20	1	1	0.775	60	−60	0	3.5	5

Below we can see the parameters entered into the subroutine "Patient" to obtain the values of compliance and the inspiratory/expiratory resistance of the respiratory system, as set out in Table 10. Again, the airway resistance simulation code, which is shown in Appendix A, and the equations presented in Section 4, have been employed for this end.

Table 10. Parameters set in the subroutine "Patient" concerning simulations of real-life cases of the Case 3.

		Parameters					
		Piston Area (A) m^2	**Spring Stiffness (k) N/m**	**Spring Pre-Compression (x_0) m**	**Cylinder Dead Volume (V_0) L**	**Restriction Area to Simulate the Inspiratory Resistance ($A_{r,i}$) m^2**	**Restriction Area to Simulate the Expiratory Resistance ($A_{r,e}$) m^2**
VC-CMV	A	0.01	196	0.0255	0.255	0.0003478	0.0001797
	B	0.01	490	0.0102	0.102	0.0003478	0.0001797
	C	0.01	196	0.0255	0.255	0.0001466	0.0001466
PC-CMV	A	0.01	490	0.0102	0.102	0.0002328	0.0002328
	B	0.01	196	0.0255	0.255	0.0001466	0.0001466

The predicted time history of the pressure upstream of the patient, flow rate inspired (>0) and expired (<0), and tidal volume, as the resistance and compliance changes, are shown in Appendix A. The relative comparison between the real-life data and the simulation data is shown in Figure 27. Again, the comparison shows that the numerical predictions are in almost perfect agreement with the real-life quantitative trend as, once again, the percentage error is less than 10%. However, the percentage error between the real-life and numerical waveforms is higher than 10% in the first phase of expiration in the pressure waveforms of the VC-CMV mode. This is caused by the extremely high accuracy of the PID controller used in the Simulink model. Indeed, the simulation results show that the airway pressure dropped instantaneously in order to the set PEEP value after the inspiration phase. Conversely, the airway pressure required a slight transitional time to reach the set PEEP value in the real-life experiments.

Changes in respiratory resistance and compliance are best visualised in the P–V loops, although there are predictable changes that occur in the F–V loops. As presented in Figure 28, during the VC-CMV mode, peak inspiratory pressure increases as compliance decreases or inspiratory resistance increases, inspiratory peak flows and tidal volumes remain similar, and expiratory peak flow decreases as lung compliance or expiratory resistance increases. Indeed, an increase in compliance is associated with a decrease in the elastic recoil of the lungs. The less elastic recoil present, the less stored energy available to be released during expiration. On the other hand, during the PC-CMV mode, tidal volume increases as lung compliance and inspiratory resistance increase, whereas inspiratory and expiratory peak flows are reduced. Furthermore, the time required for flow to reach 0 during inspiration and expiration increases.

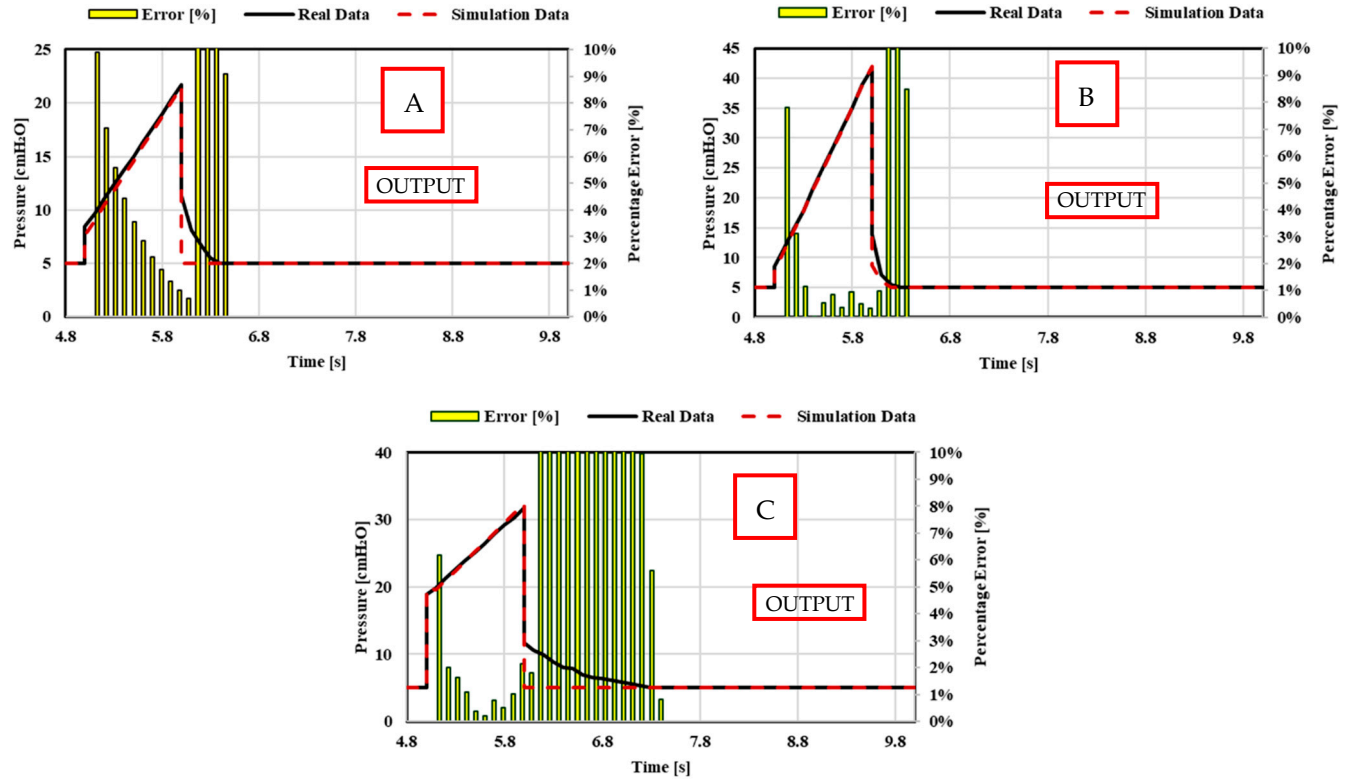

(**a**)

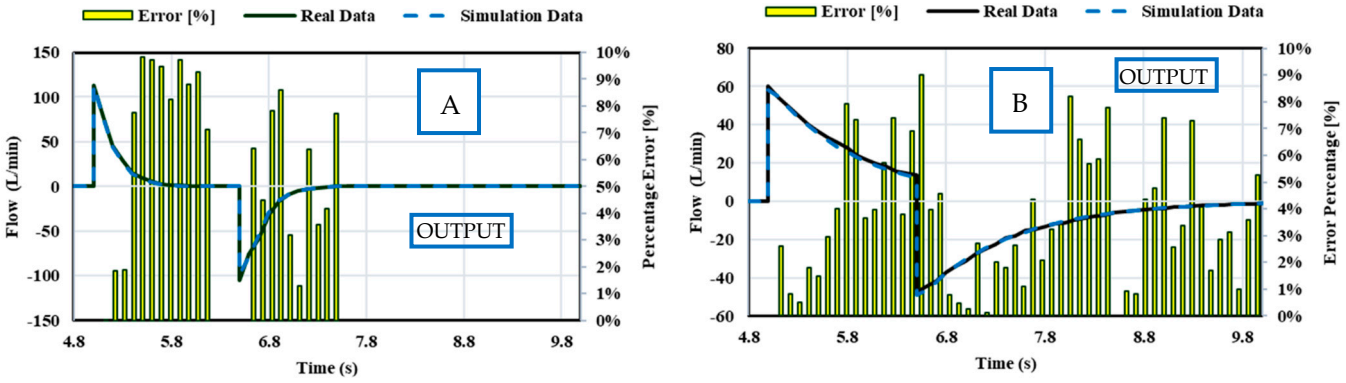

(**b**)

Figure 27. Case 3. Comparison between theoretical real-life data and simulation data for the resistance and compliance changes: (**a**) VC-CMV mode ([A] C_{RS} = 0.05 L/cmH_2O, R_{insp} = 5 cmH_2O/L/s, R_{exp} = 15 cmH_2O/L/s; [B] C_{RS} = 0.02 L/cmH_2O, R_{insp} = 5 cmH_2O/L/s, R_{exp} = 15 cmH_2O/L/s; [C] C_{RS} = 0.05 L/cmH_2O, $R_{insp/exp}$ = 20 cmH_2O/L/s); (**b**) PC-CMV mode ([A] C_{RS} = 0.02 L/cmH_2O, $R_{insp/exp}$ = 10 cmH_2O/L/s; [B] C_{RS} = 0.05 L/cmH_2O, $R_{insp/exp}$ = 20 cmH_2O/L/s).

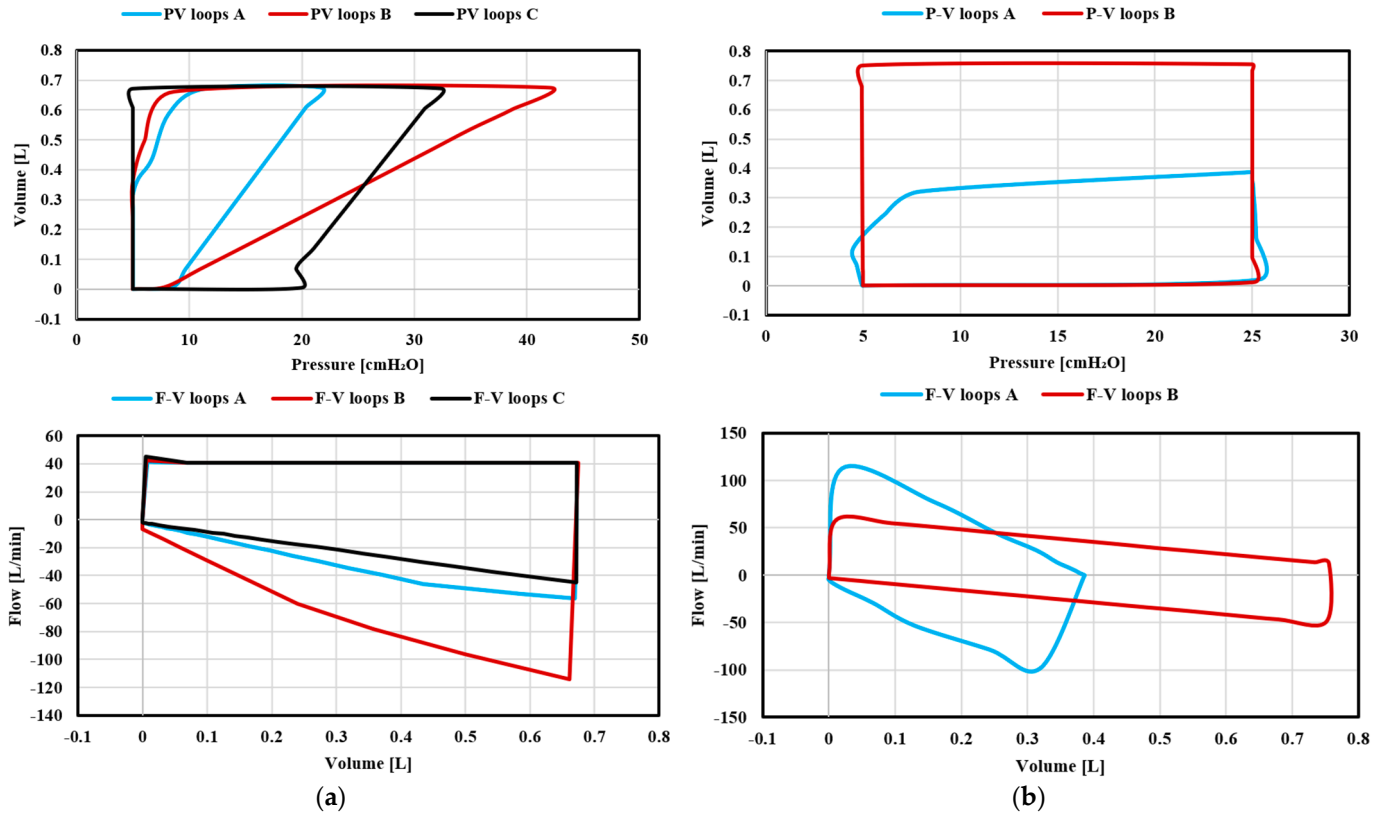

Figure 28. Case 3. Simulation results of P–V loops and F–V loops: (**a**) VC-CMV mode; (**b**) PC-CMV mode.

8. Conclusions

This paper evaluates in detail the two control modes of ventilation available to patients in intensive care units. The equations that form the basis of these typical modes of ventilation have been analysed and described in order to understand and interpret the data and the real-life waveforms taken from literature.

Two numerical codes, available via the link provided in [48], were obtained in MathWorks® Simulink software using the Simscape Fluids (gas) library, which allows the simulation of various patients with differing characteristics of lung compliance and inspiratory/expiratory resistance.

The simulation results in terms of pressure, tidal volume, and flow waveform were compared with those taken from real-life quantitative trends recorded in the scientific literature in order to validate the models. The comparisons highlighted the effectiveness and accuracy of the numerical codes, as the results demonstrated strong agreement with the real-life trends, namely by consistently reporting percentage errors of less than 10%.

In this way, the proposed codes can be used by manufacturers and start-ups in order to produce new mechanical ventilators in the shortest possible time, a vital component of critical care services for patients during the current pandemic.

Possible further improvements to this work might include:

- The analysis of the assisted–controlled ventilation modes that are employed for those patients who, despite having respiratory difficulties, are sometimes able to begin the inspiration phase independently. Therefore, the mechanical ventilator should be aware of the patient's effort to inhale and facilitate it through the function of the inspiratory trigger. This would be made possible by including the inspiration effort of the patient into the simulation code by means of a controller, thus making the ventilator able to recognise this effort and provide the respiratory act;

- The addition of a mathematical model in the VC-CMV simulation code that takes into account compliance changes during inspiration, (i.e., stress index variation), in order to reduce the percentage error between the numerical predictions and real-life data;
- The possible use of the exponential rise in pressure pattern in the PC-CMV simulation code in order to make the model more accurate.

Author Contributions: Conceptualisation, P.T., F.S., E.D., L.D.L. and R.A.; methodology, P.T., F.S., E.D., L.D.L. and R.A.; software, P.T., F.S., E.D., L.D.L. and R.A.; writing, P.T., F.S., E.D., L.D.L. and R.A. All authors have read and agreed to the published version of the manuscript.

Funding: This research received no external funding.

Data Availability Statement: The simulation code is available at: https://drive.google.com/drive/folders/1HM67XfqYSK4togaiFIuD3qpaWvFapPqG?usp=sharing (accessed on 28 October 2021).

Conflicts of Interest: The authors declare no conflict of interest.

Appendix A

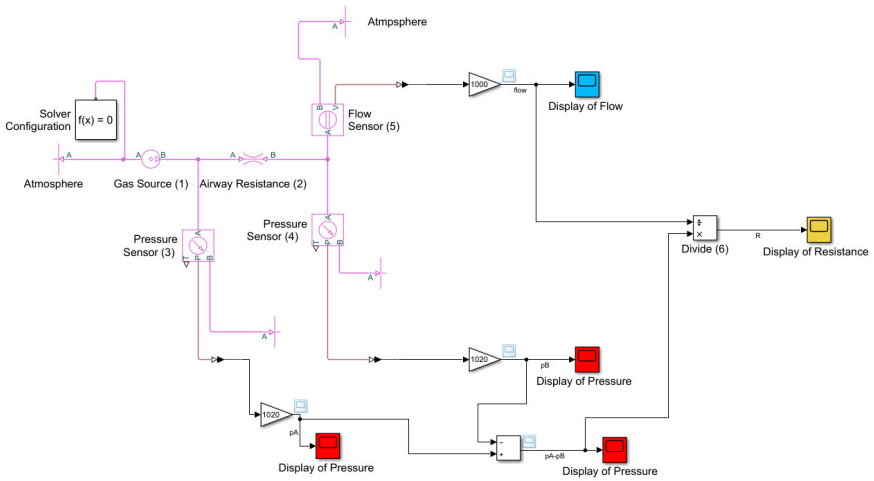

Figure A1. Airway resistance simulation code.

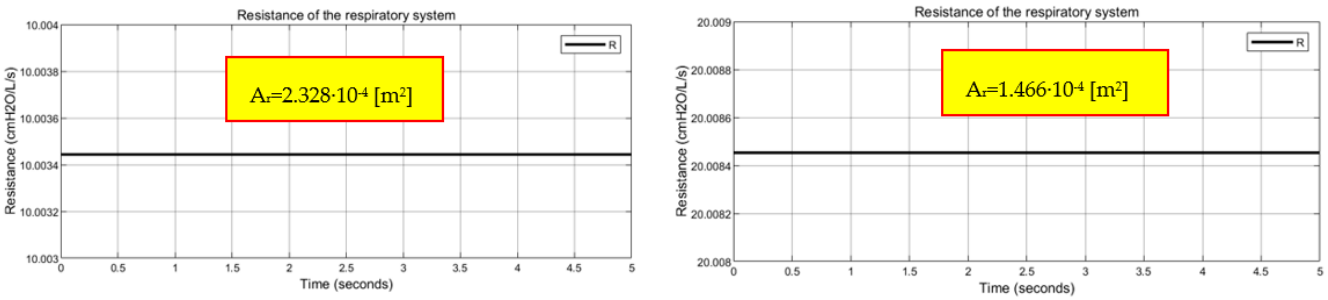

Figure A2. Resistance values of the respiratory obtained through the airway resistance simulation code.

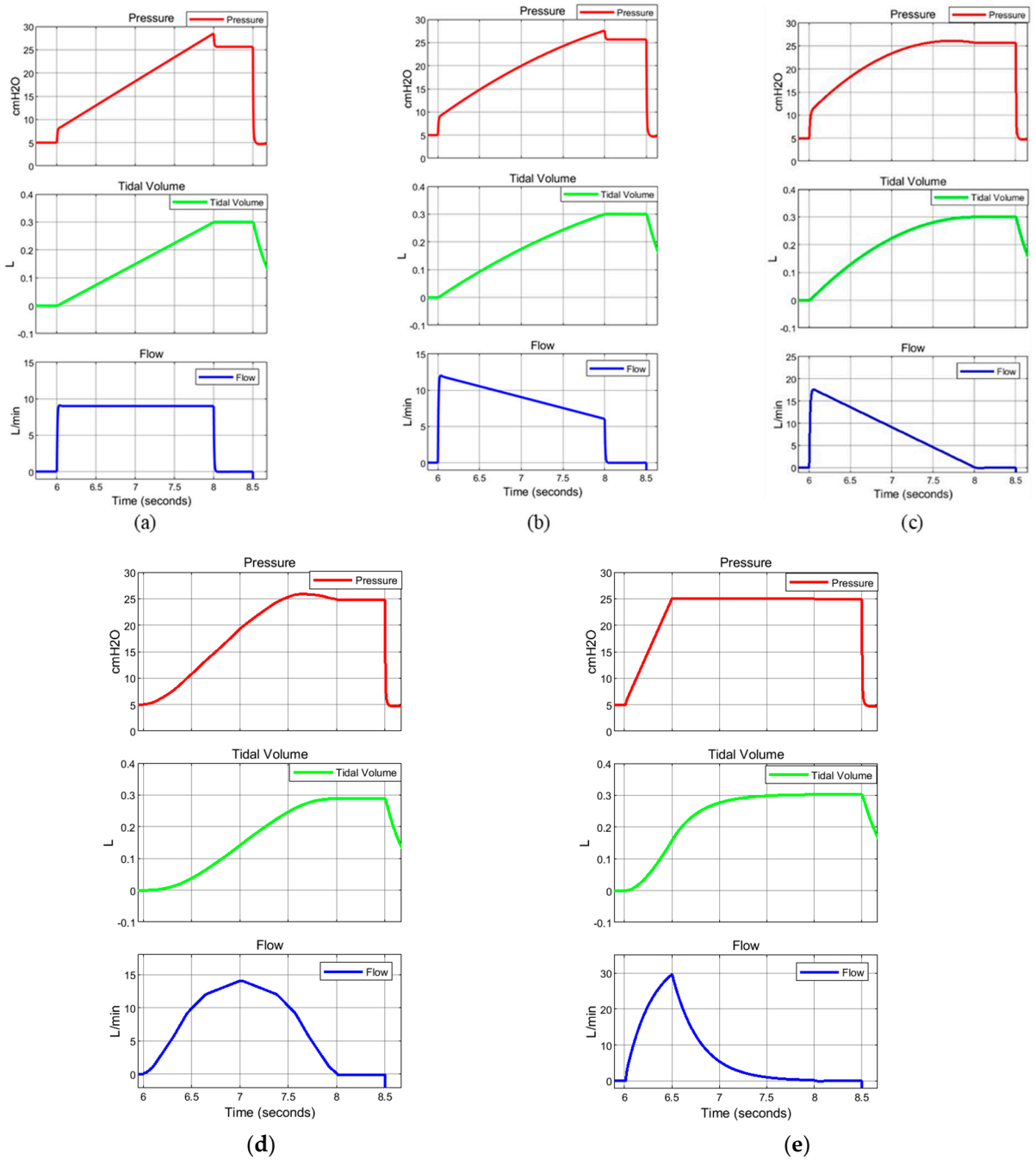

Figure A3. Case 1. Simulation results of VC-CMV and PC-CMV modes in terms of pressure, tidal volume, and inspiratory flow for different inspiratory flow patterns: (**a**) square flow, (**b**) half decelerating, (**c**) full decelerating, (**d**) sinus waveform; and for a inspiratory pressure pattern: (**e**) ramp.

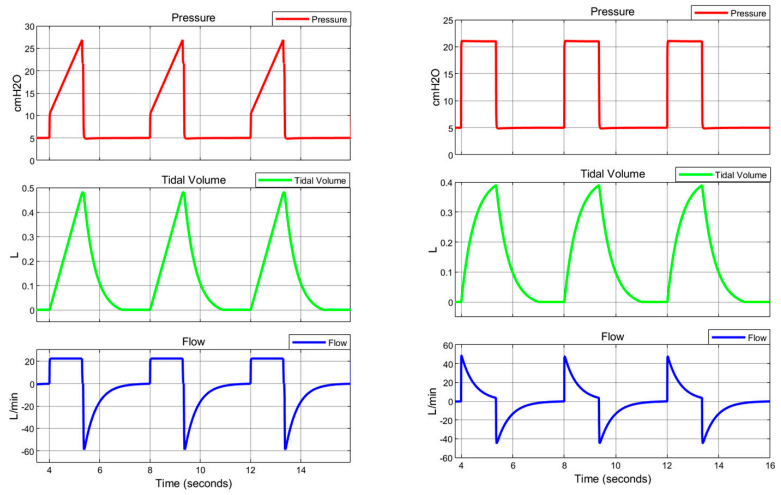

Figure A4. Case 2. Simulation results in terms of pressure, tidal volume, and inspiratory flow: (**a**) VC-CMV mode, (**b**) PC-CMV mode.

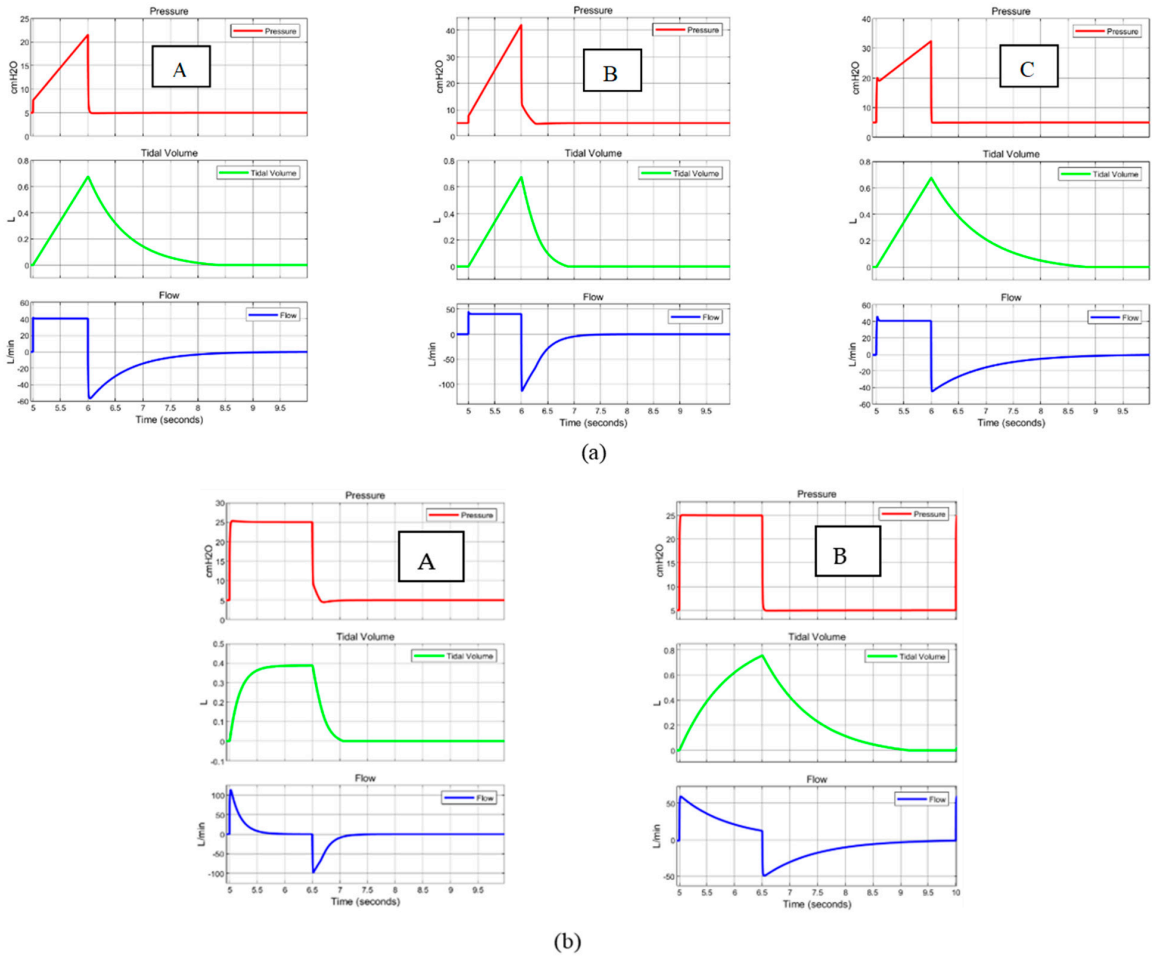

Figure A5. Case 3. Simulation results concerning the resistance and compliance changes in terms of pressure, tidal volume, and inspiratory flow: (**a**) VC-CMV mode ([A] C_{RS} = 0.05 L/cmH_2O, R_{insp} = 5 cmH_2O/L/s, R_{exp} = 15 cmH_2O/L/s; [B] C_{RS} = 0.02 L/cmH_2O, R_{insp} = 5 cmH_2O/L/s, R_{exp} = 15 cmH_2O/L/s; [C] C_{RS} = 0.05 L/cmH_2O, $R_{insp/exp}$ = 20 cmH_2O/L/s); (**b**) PC-CMV mode ([A] C_{RS} = 0.02 L/cmH_2O, $R_{insp/exp}$ = 10 cmH_2O/L/s; [B] C_{RS} = 0.05 L/cmH_2O, $R_{insp/exp}$ = 20 cmH_2O/L/s).

References

1. Kobokovich, A. *Ventilator Stockpiling and Availability in the US*; Center for Health Security: Baltimore, MD, USA, 2020.
2. Angulo, M.; Beltramelli, R.; Amarelle, L.; Alzugaray, P.; Briva, A.; Santos, C. Mechanical Risks of Ventilator Sharing in the COVID-19 Era: A Simulation-Based Study. *Arch. Bronconeumol.* **2020**, *56*, 752. [CrossRef] [PubMed]
3. Solís-Lemus, J.A.; Costar, E.; Doorly, D.; Kerrigan, E.C.; Kennedy, C.H.; Tait, F.; Niderer, S.; Vincent, P.E.; Williams, S.E. A simulated single ventilator/dual patient ventilation strategy for acute respiratory distress syndrome during the COVID-19 pandemic. *R. Soc. Open Sci.* **2020**, *7*, 200585. [CrossRef] [PubMed]
4. Pedersen, J.M.; Jebaei, F.; Jradi, M. Assessment of Building Automation and Control Systems in Danish Healthcare Facilities in the COVID-19 Era. *Appl. Sci.* **2022**, *12*, 427. [CrossRef]
5. Campanini, M.; Lari, F.; Giorgi Pierfranceschi, M. La ventilazione non invasiva in Medicina Interna. *Ital. J. Med.* **2015**, *3*, 391–498.
6. Walter, J.M.; Corbridge, T.C.; Singer, B.D. Invasive mechanical ventilation. *South. Med. J.* **2018**, *111*, 746. [CrossRef]
7. Martin, J.T. *Principles and Practice of Mechanical Ventilation*; The McGraw-Hill Companies Inc.: New York, NY, USA, 2013.
8. Cairo, J.M. *Pilbeam's Mechanical Ventilation: Physiological and Clinical Applications*; Elsevier Health Sciences: St. Louis, MO, USA, 2015.
9. Hickey, S.M.; Giwa, A.O. *Mechanical Ventilation*; StatPearls Publishing: Treasure Island, FL, USA, 2020.
10. Santanilla, J.I.; Daniel, B.; Yeow, M.E. Mechanical ventilation. *Emerg. Med. Clin. North Am.* **2008**, *26*, 849–862. [CrossRef]
11. Censi, F.; Calcagnini, G.; Mattei, E.; Triventi, M.; Bartolini, P. Tecnologie wireless e dispositivi medici: Aspetti normativi riguardanti la compatibilità elettromagnetica. *Dell'istituto Superiore di Sanità dell'Istituto Superiore di Sanità* **2010**, *23*, 11–16.
12. GALILEO Service Manual. Available online: https://www.hamilton-medical.com (accessed on 5 June 2021).
13. Dräger Infinity V500 Manual. Available online: https://www.draeger.com/en-us_us/Products/Evita-Infinity-V500-ventilator (accessed on 5 June 2021).
14. Aisys CS^2 User's Reference Manual. Available online: http://www3.gehealthcare.it/ (accessed on 5 June 2021).
15. Operator's and Technical Reference Manual of Puritan Bennett 800 Series Ventilator System. Available online: https://www.medtronic.com/ (accessed on 5 June 2021).
16. Specification for Rapidly Manufactured Ventilator System (RMVS). Issued by MHRA (2020). Available online: https://assets.publishing.service.gov.uk/government/uploads/system/uploads/attachment_data/file/879382/RMVS001_v4.pdf (accessed on 5 June 2021).
17. Arnal, J.M.; Garnero, A.; Saoli, M.; Chatburn, R.L. Parameters for simulation of adult subjects during mechanical ventilation. *Respir. Care* **2018**, *63*, 158–168. [CrossRef]
18. Mojoli, F.; Iotti, G.A.; Arnal, J.M.; Braschi, A. Is the ventilator switching from inspiration to expiration at the right time? Look at waveforms! *Intensive Care Med.* **2016**, *42*, 914–915. [CrossRef]
19. Galbiati, C.; Abba, A.; Agnes, P.; Amaudruz, P.; Arba, M.; Ardellier-Desages, F.; Badia, C.; Batignani, G.; Bellani, G.; Bianchi, G.; et al. Mechanical Ventilator Milano (MVM): A novel mechanical ventilator designed for mass scale production in response to the COVID-19 pandemics. *arXiv* **2020**, arXiv:2003.10405.
20. Maggiali, M.; Crepaldi, M.; Pattacini, U.; Onorato, C. *FI5 Ventilator*; Istituto Italiano di Tecnologia: Genova, Italy, 2020.
21. Grasselli, G.; Cattaneo, E.; Florio, G.; Ippolito, M.; Zanella, A.; Cortegiani, A.; Huang, J.; Pesenti, A.; Einav, S. Mechanical ventilation parameters in critically ill COVID-19 patients: A scoping review. *Crit. Care* **2021**, *25*, 1–11. [CrossRef] [PubMed]
22. Botta, M.; Tsonas, A.M.; Pillay, J.; Boers, L.S.; Algera, A.G.; Bos, L.D.; Dongelmans, D.A.; Hollmann, M.W.; Horn, J.; Vlaar, A.P.J.; et al. Ventilation management and clinical outcomes in invasively ventilated patients with COVID-19 (PRoVENT-COVID): A national, multicentre, observational cohort study. *Lancet Respir. Med.* **2021**, *9*, 139–148. [CrossRef]
23. Cavayas, Y.A.; Noël, A.; Brunette, V.; Williamson, D.; Frenette, A.J.; Arsenault, C.; Bellamare, P.; Lagrenade-Verdant, C.; LeGuillan, S.; Levesque, E.; et al. Early experience with critically ill patients with COVID-19 in Montreal. *Can. J. Anesth. J. Can. D'anesthésie* **2021**, *68*, 204–213. [CrossRef] [PubMed]
24. Sinha, P.; Calfee, C.S.; Cherian, S.; Brealey, D.; Cutler, S.; King, C.; Killick, C.; Richards, O.; Cheema, Y.; Bailey, C.; et al. Prevalence of phenotypes of acute respiratory distress syndrome in critically ill patients with COVID-19: A prospective observational study. *Lancet Respir. Med.* **2020**, *8*, 1209–1218. [CrossRef]
25. Bos, L.D.; Paulus, F.; Vlaar, A.P.; Beenen, L.F.; Schultz, M.J. Subphenotyping acute respiratory distress syndrome in patients with COVID-19: Consequences for ventilator management. *Ann. Am. Thorac. Soc.* **2020**, *17*, 1161–1163. [CrossRef]
26. Diehl, J.L.; Peron, N.; Chocron, R.; Debuc, B.; Guerot, E.; Hauw-Berlemont, C.; Hermann, B.; Augy, J.L.; Younan, R.; Novara, A.; et al. Respiratory mechanics and gas exchanges in the early course of COVID-19 ARDS: A hypothesis-generating study. *Ann. Intensive Care* **2020**, *10*, 1–7. [CrossRef]
27. Grasselli, G.; Tonetti, T.; Protti, A.; Langer, T.; Girardis, M.; Bellani, G.; Laffey, J.; Carrafiello, G.; Carsana, L.; Rizzuto, C.; et al. Pathophysiology of COVID-19-associated acute respiratory distress syndrome: A multicentre prospective observational study. *Lancet Respir. Med.* **2020**, *8*, 1201–1208. [CrossRef]
28. Bonci, A.; De Amicis, R.; Longhi, S.; Scala, G.A.; Andreucci, A. Motorcycle lateral and longitudinal dynamic modeling in presence of tyre slip and rear traction. In Proceedings of the 2016 21st International Conference on Methods and Models in Automation and Robotics (MMAR), Miedzyzdroje, Poland, 29 August–1 September 2016; pp. 391–396.

29. Bonci, A.; De Amicis, R.; Longhi, S.; Lorenzoni, E.; Scala, G.A. A motorcycle enhanced model for active safety devices in intelligent transport systems. In Proceedings of the 2016 12th IEEE/ASME International Conference on Mechatronic and Embedded Systems and Applications (MESA), Auckland, New Zealand, 29–31 August 2016; pp. 1–6.
30. Bonci, A.; Longhi, S.; Scala, G.A. Towards an all-wheel drive motorcycle: Dynamic modeling and simulation. *IEEE Access* **2020**, *8*, 112867–112882. [CrossRef]
31. Hernández-Santos, C.; Davizón, Y.A.; Said, A.R.; Soto, R.; Felix-Herrán, L.C.; Vargas-Martínez, A. Development of a Wearable Finger Exoskeleton for Rehabilitation. *Appl. Sci.* **2021**, *11*, 4145. [CrossRef]
32. Yahya, Y.Z.; Al-Sawaff, Z.H. Design and Modeling of An Upper Limb Exoskeleton to Assist Elbow Joint Movement Using Surface Emg Signals. *Biomed. Eng. Appl. Basis Commun.* **2020**, *32*, 2050006. [CrossRef]
33. Zhang, G.; Wang, J.; Yang, P.; Guo, S. Iterative learning sliding mode control for output-constrained upper-limb exoskeleton with non-repetitive tasks. *Appl. Math. Model.* **2021**, *97*, 366–380. [CrossRef]
34. Giri, J.; Kshirsagar, N.; Wanjari, A. Design and simulation of AI-based low-cost mechanical ventilator: An approach. *Mater. Today Proc.* **2021**, *47*, 5886–5891. [CrossRef] [PubMed]
35. Guler, H.; Ata, F. Design of a fuzzy-LabVIEW-based mechanical ventilator. *Comput. Syst. Sci. Eng.* **2014**, *29*, 219–229.
36. Pasteka, R.; Santos da Costa, J.P.; Barros, N.; Kolar, R.; Forjan, M. Patient–Ventilator Interaction Testing Using the Electromechanical Lung Simulator xPULM™ during V/AC and PSV Ventilation Mode. *Appl. Sci.* **2021**, *11*, 3745. [CrossRef]
37. Pasteka, R.; Forjan, M.; Sauermann, S.; Drauschke, A. Electro-mechanical lung simulator using polymer and organic human lung equivalents for realistic breathing simulation. *Sci. Rep.* **2019**, *9*, 1–12.
38. El-Hadj, A.; Kezrane, M.; Ahmad, H.; Ameur, H.; Abd Rahim, S.Z.B.; Younsi, A.; Abu-Zinadah, H. Design and simulation of mechanical ventilators. *Chaos Solitons Fractals* **2021**, *150*, 111169. [CrossRef] [PubMed]
39. Simulink Documentation, The MathWorks, Inc. 2019. Available online: https://www.mathworks.com/help/simulink/ (accessed on 1 June 2021).
40. Matlab & Simulink. *SimscapeTM User's Guide R2019a*; The MathWorks, Inc.: Natick, MA, USA, 2019.
41. Chatburn, R.L.; El-Khatib, M.; Mireles-Cabodevila, E. A taxonomy for mechanical ventilation: 10 fundamental maxims. *Respir. Care* **2014**, *59*, 1747–1763. [CrossRef] [PubMed]
42. Chatburn, R.L. Classification of ventilator modes: Update and proposal for implementation. *Respir. Care* **2007**, *52*, 301–323.
43. Kacmarek, R.M.; Stoller, J.K.; Heuer, A. *Egan's Fundamentals of Respiratory Care E-Book*; Elsevier Health Sciences: St. Louis, MO, USA, 2019.
44. Chatburn, R.L.; Lough, M.D. Mechanical ventilation. In *Pediatric Respiratory Therapy*, 3rd ed.; Mandu Press LTD: Cleveland, OH, USA, 2003.
45. Correger, E.; Murias, G.; Chacon, E.; Estruga, A.; Sales, B.; Lopez-Aguilar, J.; Montanya, J.; Lucangelo, U.; Garcia-Esquirol, O.; Villagra, A.; et al. Interpretation of ventilator curves in patients with acute respiratory failure. *Med. Intensiva Engl. Ed.* **2012**, *36*, 294–306. [CrossRef]
46. Pupella, R.A. *Mechanical Ventilation in Patient with Respiratory Failure*; Springer: Singapore, 2018.
47. Al Ashry, H.S.; Modrykamien, A.M. Humidification during mechanical ventilation in the adult patient. *BioMed Res. Int.* **2014**, *2014*, 715434. [CrossRef]
48. Available online: https://drive.google.com/drive/folders/1HM67XfqYSK4togaiFIuD3qpaWvFapPqG?usp=sharing (accessed on 28 October 2021).
49. Hess, D.; Kacmarek, R.M. *Essentials of Mechanical Ventilation*; McGraw Hill Education: New York, NY, USA, 2014.